nagra.

Technical Report 08-12

Corrosion of carbon steel under anaerobic conditions in a repository for SF and HLW in Opalinus Clay

October 2008

Fraser King

Integrity Corrosion Consulting Ltd.

National Cooperative
for the Disposal of
Radioactive Waste

Hardstrasse 73
CH-5430 Wettingen
Switzerland
Tel. +41 56 437 11 11

www.nagra.ch

nagra.

Technical Report 08-12

Corrosion of carbon steel under anaerobic conditions in a repository for SF and HLW in Opalinus Clay

October 2008

Fraser King

Integrity Corrosion Consulting Ltd.

Integrity Corrosion Consulting Ltd.
3396 Stephenson Point Road
Nanaimo, BC, Canada V9T 1K2

National Cooperative
for the Disposal of
Radioactive Waste

Hardstrasse 73
CH-5430 Wettingen
Switzerland
Tel. +41 56 437 11 11

www.nagra.ch

This report was prepared on behalf of Nagra. The viewpoints presented and conclusions reached are those of the author(s) and do not necessarily represent those of Nagra.

ISSN 1015-2636

Abstract

Nagra is considering carbon steel as one of the canister material options for the disposal of high-level waste and spent fuel in a deep geological repository in Opalinus Clay. Following a brief period of aerobic conditions, the canister will be exposed to an anaerobic environment for much of its service life. Knowledge of the rate of anaerobic corrosion is important not only for estimating the canister lifetime but also for determining the rate of hydrogen generation.

This report describes a critical review of the anaerobic corrosion behaviour of carbon steel under environmental conditions similar to those expected in the repository. The aims of the report are:

1. to recommend a (range of) long-term anaerobic corrosion rate(s) for carbon steel canisters, and
2. to justify the use of this rate in safety assessments based on a mechanistic understanding of the structure and properties of the protective corrosion product films.

The review is based on selected studies from various national nuclear waste management programs, supplemented where appropriate with studies from other applications and with evidence from archaeological analogues.

The corrosion rate of carbon steel decreases with time because of the formation of a protective surface film. There are differences in behaviour in bulk solution and in the presence of compacted bentonite. In bulk solution, the corrosion rate decreases to an apparent steady-state rate after a period of approximately six months, with a long-term rate of the order of 0.1 μm·yr. The surface film comprises a duplex structure, with a magnetite outer layer and a spinel-type inner layer. In compacted clay systems the rate of decrease in corrosion rate is slower, with steady-state not being reached after several years of exposure. There is a significant body of evidence from apparently well-conducted experiments that indicate an anaerobic corrosion rate of the order of $1 – 2$ μm·yr^{-1} in systems containing compacted clay and the protective films tend to be carbonate-based rather than magnetite-based.

There is no evidence in the literature that the use of a constant long-term corrosion rate for safety assessment purposes is not justified. Factors that are important in determining the structure and properties of the corrosion product film are reviewed, including the effects of the aerobic-anaerobic transition on the film composition and structure, possible spalling of protective films, and the effect of the accumulation of corrosion products on the corrosion rate of the underlying steel.

Zusammenfassung

Für die Entsorgung hochaktiver Abfälle und abgebrannter Brennelemente in einem geologischen Tiefenlager im Opalinuston zieht die Nagra Kohlenstoffstahl als eine der Materialoptionen für den Endlagerbehälter in Betracht. Nach einer kurzen Periode in einer aeroben Umgebung werden die Behälter für den Grossteil ihrer Lebensdauer anaeroben Bedingungen ausgesetzt sein. Kenntnis der anaeroben Korrosionsrate ist nicht nur wichtig, um die Behälterlebensdauer abzuschätzen, sondern auch, um die Produktionsrate von Wasserstoff zu bestimmen.

Dieser Bericht enthält einen kritischen Review des anaeroben Korrosionsverhaltens von Kohlenstoffstahl unter Bedingungen, wie sie im Tiefenlager erwartet werden. Die Ziele des Berichtes sind

1. eine anaerobe Langzeit-Korrosionsrate für Kohlenstoffstahlbehälter vorzuschlagen, und
2. basierend auf einem mechanistischen Verständnis der Struktur und der Eigenschaften des Korrosionsproduktefilms die Verwendung dieser Langzeit-Korrosionsrate in Sicherheitsanalysen zu rechtfertigen.

Der Review basiert auf ausgewählten Studien aus verschiedenen nationalen Entsorgungsprogrammen, die, wo angemessen, durch Studien aus anderen Gebieten und mit Hinweisen aus archäologischen Analoga ergänzt wurden.

Die Korrosionsgeschwindigkeit von Kohlenstoffstahl nimmt aufgrund der Bildung eines schützenden Films aus Korrosionsprodukten mit der Zeit ab. Das Korrosionsverhalten ist unterschiedlich in Wasser und in wassergesättigtem kompaktiertem Bentonit. In Wasser nähert sich die Korrosionsgeschwindigkeit nach ungefähr sechs Monaten einer scheinbaren (“apparent”) stationären Langzeitrate in der Grössenordnung von 0.1 $\mu m \cdot a^{-1}$. Der Korrosionsproduktefilm besteht aus einer Doppelstruktur mit einer äusseren Magnetitschicht und einer inneren spinellartigen Schicht. In kompaktierten Tonsystemen nimmt die Korrosionsgeschwindigkeit langsamer ab und eine stationäre Rate ist selbst nach einigen Jahren noch nicht erreicht. Eine signifikante Anzahl von qualitativ hochwertigen Experimenten weist auf eine anaerobe Korrosionsgeschwindigkeit hin in der Grössenordnung von $1 – 2\ \mu m \cdot a^{-1}$ für Systeme in einer Umgebung in wassergesättigtem kompaktiertem Ton, und die schützenden Korrosionsproduktefilme sind tendenziell karbonathaltig anstatt magnetithaltig.

Es gibt keine Hinweise in der Literatur, dass die Verwendung einer konstanten Langzeit-Korrosionsrate in Sicherheitsanalysen nicht gerechtfertigt ist. Faktoren, die bei der Bestimmung der Struktur und Eigenschaften des Korrosionsproduktefilms wichtig sind, werden bewertet, einschliesslich der Auswirkungen des Übergangs von aeroben zu anaeroben Bedingungen auf die Zusammensetzung und Struktur des Films, das mögliche Abplatzen des schützenden Films sowie die Auswirkung der Akkumulation von Korrosionsprodukten auf die Korrosionsraten des darunterliegenden Stahls.

Résumé

L'acier au carbone est l'un des matériaux envisagés par la Nagra pour les conteneurs destinés au stockage des déchets de haute activité et des éléments combustibles usés dans un dépôt en couches géologiques profondes situé dans les Argiles à Opalinus. A l'issue d'une brève période aérobie, le conteneur se trouvera dans des conditions anaérobies pour la plus grande part de sa durée d'utilisation. Le taux de corrosion anaérobie est important non seulement pour estimer la durée de vie du conteneur, mais aussi pour déterminer le taux de production d'hydrogène.

Le présent rapport fait le point sur la corrosion anaérobie de l'acier au carbone dans des conditions similaires à celles qui régneront dans le dépôt. Ses objectifs sont les suivants:

1. recommander un taux (ou une fourchette de taux) relatif à la corrosion anaérobie à long terme des conteneurs en acier au carbone et
2. justifier l'usage de ce taux dans les analyses de sûreté basées sur une approche mécanistique de la structure et des propriétés des films protecteurs composés de produits de corrosion.

Un choix d'études réalisées dans le cadre de différents programmes d'évacuation des déchets radioactifs ont été consultées et complétées si nécessaire par des expériences émanant d'autres applications et des démonstrations apportées par les analogues archéologiques.

Le taux de corrosion de l'acier au carbone décroît en fonction du temps en raison de la formation d'un film protecteur à la surface de l'acier. Des différences ont été observées selon que l'environnement comportait ou non de la bentonite compactée. Dans un environnement sans argile compactée, la réaction de corrosion se ralentit progressivement au cours d'une période d'environ six mois jusqu'à atteindre un état stable en apparence, le taux de corrosion à long terme étant de l'ordre de 0.1 μm par an. Le film de surface se compose alors de magnétite doublée à l'intérieur d'une couche de type spinelle. Dans les systèmes d'argiles compactées, le taux de corrosion décroît plus lentement, une stabilisation n'intervenant qu'après plusieurs années. Des données expérimentales apparemment fiables semblent indiquer un taux de corrosion anaérobie de l'ordre de $1 – 2\ \mu m \cdot a^{-1}$ en présence de bentonite compactée. Ici, les films protecteurs paraissent contenir du carbonate plutôt que de la magnétite.

Si l'on se base sur les études consultées, il ne semble pas y avoir d'objection à l'utilisation d'un taux de corrosion à long terme constant dans le cadre des analyses de sûreté. Le rapport passe en outre en revue les facteurs influant sur la structure et les propriétés du film protecteur, notamment les effets du passage de conditions aérobies à des conditions anaérobies sur la composition et la structure du film, l'éventuel écaillage du film protecteur, ainsi que l'effet de l'accumulation des produits de corrosion sur le taux de corrosion de l'acier sous-jacent.

Table of Contents

List of Tables

List of Figures

1 Introduction

Nagra is considering carbon steel (C-steel) as one option for a canister material for the disposal of high-level waste (HLW) and spent fuel (SF) in a deep geologic repository in Opalinus Clay (Nagra 2002). Carbon steel is an attractive material for this purpose because of the relative ease and flexibility of fabrication, good corrosion performance, extensive industrial experience, and relatively low cost.

The present review of the long-term corrosion mechanism and rate of carbon steel under conditions relevant to disposal of HLW and SF in a repository in Opalinus Clay was performed in order to provide input to Nagra's discussions with its Canister Materials Review Board. The Board was convened as a result of the recommendations of the authorities regarding the options for canister materials arising from the review of Project Entsorgungsnachweis (Nagra 2002). The recommendations of the authorities and Nagra's plan for dealing with them in the context of the next stages of repository development are discussed in Nagra (2008). The findings of the Board, including its assessment of carbon steel and other possible canister materials, as well as their recommendations for future work, are given in Landolt et al. (2009).

The Opalinus Clay is a low permeability Jurassic claystone with a thickness of about 110 m. The carbon steel canisters, with a wall thickness of 13 – 15 cm, would be horizontally emplaced with their supporting bentonite blocks in excavated tunnels (diameter 2.5 m). After each canister is emplaced, the voids around and between canisters would be filled with a granular bentonite mixture prepared from dense bentonite pellets. The bentonite would gradually take up water from the host rock, swell and form a low permeability barrier around the canisters, with full complete saturation taking about 50 to 100 years. Rock mechanics and tunnelling experience in Opalinus Clay suggest that no ground support (e.g. shotcrete) is likely to be needed in the small diameter emplacement tunnels, although steel mesh and rock bolts are expected to be used.

Opalinus Clay is a claystone comprising, on average, 40 % clay minerals, 30 % carbonates and 20 – 30 % quartz plus minor accessory minerals. It has a porosity of about 12 % and a hydraulic conductivity of $< 10^{-13}$ m s^{-1}. Transport in the rock is diffusion controlled, providing effective hydraulic isolation from overlying and underlying rocks. The porewater chemistry in Opalinus Clay is brackish, with an ionic strength of 0.3 and with major ion chemistry dominated by Ca, Na, SO_4 and Cl. Redox conditions in the Opalinus Clay are considered to be strongly reducing as a result of the presence of pyrite (about 1 %) and abundant siderite in the host rock (Nagra 2002).

There are a number of regulatory, design, safety, and economic requirements for the canister. There is a regulatory requirement for a minimum canister lifetime of 1000 yrs. From a safety perspective, it would be advantageous if the canister survived for the entire initial transient period during which the thermal-hydrological-mechanical-chemical conditions in the repository are evolving, perhaps a period of several thousand years. This is a benefit in relation to reducing the complexity of models required for transient phenomena; in particular, it avoids any requirement for coupled models that include radionuclide transport. Also from a safety viewpoint, none of the barriers in the multi-barrier system, including the canister, should compromise the functioning of any other barrier. In this respect, the impact of dissolved Fe(II) on the alteration of bentonite and of H_2 generated from anaerobic corrosion of the canister need to be addressed.

Environmental conditions within the repository will evolve over time. Initially, conditions will be hot (maximum canister surface temperature of ~ 150 °C), aerobic, and relatively dry within the bentonite barrier. As the canister cools and the repository saturates with groundwater, and as

the initially trapped O_2 is consumed by corrosion and microbiological processes and by reaction with Fe(II) minerals, the repository environment will become cool and anaerobic and remain so indefinitely. The initial aerobic phase is expected to be of less than 100 yrs duration (Wersin et al. 2003). Although the nature and extent of corrosion during the initial aerobic phase are acknowledged to require some further evaluation, there are good reasons to believe that the total extent of corrosion will be small relative to the canister wall thickness (Johnson and King 2003). Given that safety assessments are required for periods of tens to hundreds of thousands of years, most of the time period of interest corresponds to the period of anaerobic conditions.

There are two main purposes for this review. First, a critical review of published anaerobic corrosion rate data is required to justify the rate, or rates, used in predicting both canister lifetimes and the rate of formation of corrosion products (for the current purposes, principally H_2). Second, the available mechanistic information regarding the structure and properties of the corrosion product film is reviewed with a view to providing justification for the use of a long-term anaerobic corrosion rate (or rates) in safety assessments. In particular, the following questions are addressed:

- what rate, or rates, should be used for the long-term corrosion of C-steel under anaerobic conditions,
- what is the mechanism of corrosion, particularly the structure of the corrosion product film and the nature of the rate-controlling process, including dissolution and transport of Fe(II) species by diffusion into the bentonite,
- qualitatively, how will the corrosion behaviour of the canister change as the environmental conditions within the repository evolve, and
- are there any processes that might lead to an increase in the corrosion (and H_2 generation) rate?

There is a large amount of published information on the corrosion of C-steel in natural environments. By necessity, therefore, the scope of this review is limited to the behaviour of C-steel under fully saturated, anaerobic conditions and at temperatures from ambient up to approximately 100 – 150 ^{o}C. Furthermore, the canisters are assumed to be self-shielding, so that effects of gamma irradiation are not considered. Information from studies performed outside this range of conditions has only been included if it provides insight into the behaviour for the conditions of interest. For corrosion rate studies, the major focus is on measurements performed in various national nuclear waste management programs, supplemented where appropriate with studies from other applications and with evidence from archaeological analogues. Mechanistic information from a wide range of applications has been reviewed and the implications for the corrosion behaviour of canisters under anaerobic conditions, and during the aerobic-anaerobic transition, considered.

2 Corrosion rate of C-steel under anaerobic conditions

As noted above, a value for the rate of anaerobic corrosion is required to both predict the lifetime of the canister and to estimate the rate of generation of H_2 and Fe(II) corrosion products. As background to this critical review of the literature, Figures 1 and 2 show the data currently used by Nagra to derive a long-term anaerobic corrosion rate (Johnson and King 2003). There are several notable features of these data:

- the rate of corrosion decreases with increasing length of exposure, based on results from both individual studies (Fig. 1) and from the compiled results of multiple studies (Fig. 2),
- comparison of different studies indicates measured rates that vary by 2 to 3 orders of magnitude (Fig. 2(b)), and
- there is no indication of an increase in corrosion rate with increasing exposure period.

Based on the data in Figures 1 and 2, a long-term anaerobic corrosion rate of 1 $\mu m \cdot yr^{-1}$ has been selected for predicting the lifetime of the canister (Johnson and King 2003). In selecting an appropriate corrosion rate, greater emphasis was placed on long-term studies (in order to properly account for the effect of film formation) and on gas-generation studies (which avoid any uncertainty due to corrosion due to incomplete deaeration of the test environment).

Despite the widespread use of C-steel in natural environments and the corresponding extensive literature, there are relatively few published studies of corrosion rates under anaerobic conditions. Many of the studies in the literature were performed under aerated, or partially aerated, conditions. Apart from the current application, the only industrial uses of C-steel in anaerobic environments that have been studied in detail are boiler feed water systems and underground pipelines. In the case of boiler feed water systems, both the temperature and pH of the environment are generally higher than those of interest here. In addition, because of the relatively high rate of mass transport, corrosion rates tend to be determined by the rate of removal of a protective Fe_3O_4 film. In the case of buried pipelines, the use of measured rates is complicated by the often poorly characterized soil conditions and, for direct measurements from the pipe, by the effects of residual coating and of the cathodic protection system. In addition, microbes are invariably involved in the corrosion of underground pipelines but, for the current application, microbial activity close to the canister is believed to not occur because of the presence of compacted bentonite clay (Stroes-Gascoyne et al. 2007). Consequently, most emphasis here is on studies from the nuclear waste management literature.

Corrosion rates reported in the nuclear waste management literature are typically determined from either the weight loss of the coupons or from measurements of the rate of H_2 evolution. Because of the decrease in rate with time due to film formation, the rates determined from these two techniques are not strictly comparable. Weight-loss corrosion rates are averaged over the entire duration of the exposure period, and are higher than the actual rate at the end of the test. For example, if the corrosion rate decreases according to $t^{-1/2}$, the time-averaged weight-loss corrosion rate is twice the instantaneous rate at any given time. Rates measured from the evolution of H_2 are more representative of "instantaneous" corrosion rates characteristic of the rate of corrosion at the time of measurement. However, even rates determined from H_2 evolution are only an approximation of the instantaneous corrosion rate as the rate is derived from the amount of H_2 evolved between successive measurements. In this report, time-averaged rates derived from weight-loss measurements are distinguished from "instantaneous" rates derived from H_2-evolution measurements. Although corrosion rates can also be determined electrochemically, it is difficult to properly account for the effects of time-dependent film formation. Consequently, electrochemically derived corrosion rates are not considered here.

The following discussion reviews various results from relevant studies of the corrosion rate of carbon steel. The details of the mechanism of corrosion and the structure and composition of the corrosion film are discussed in succeeding sections of the report.

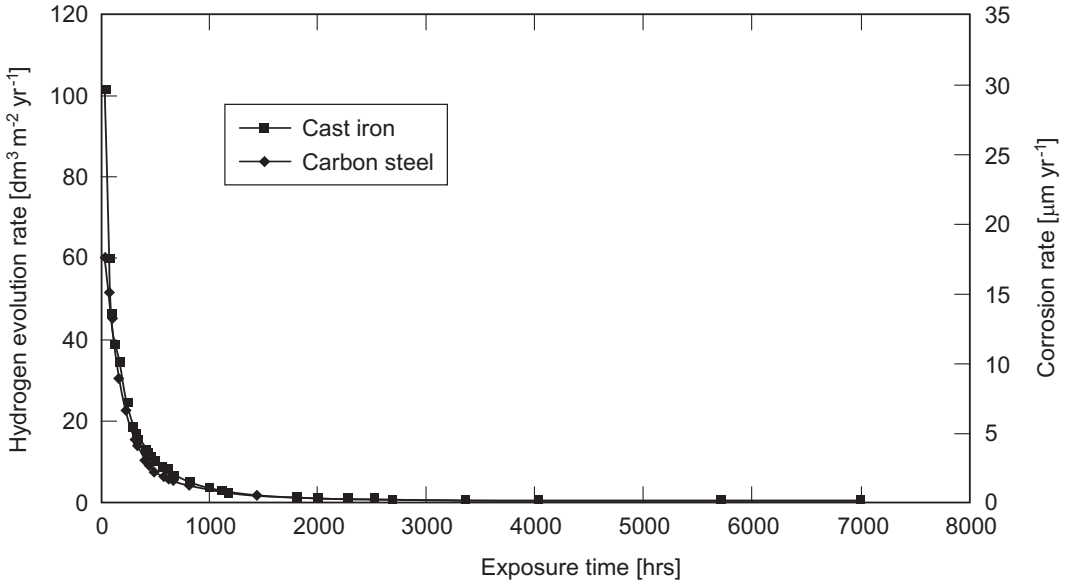

(a) corrosion rates of cast iron and carbon steel in Äspö groundwater at 85 °C (Smart et al. 2001)

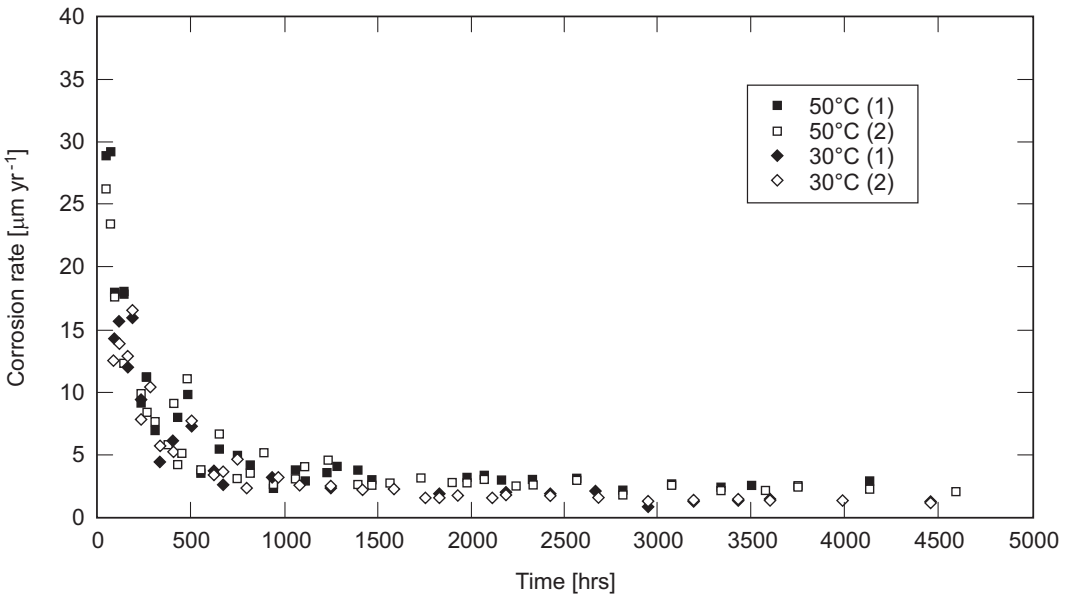

(b) corrosion rate of carbon steel in compacted bentonite saturated with 1 mol dm^{-3} NaCl at pH 8.4 (Smart et al. 2006b)

Figure 1: Time dependence of anaerobic corrosion rate of carbon steel and cast iron determined from hydrogen generation rates

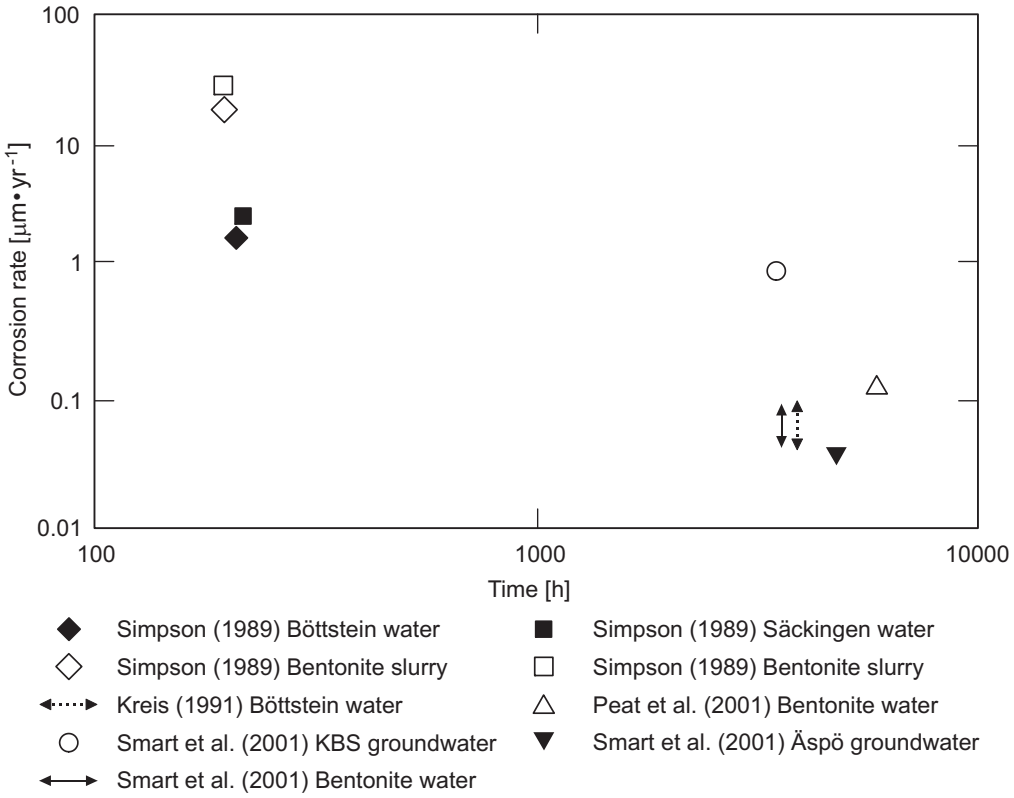

(a) Gas generation data

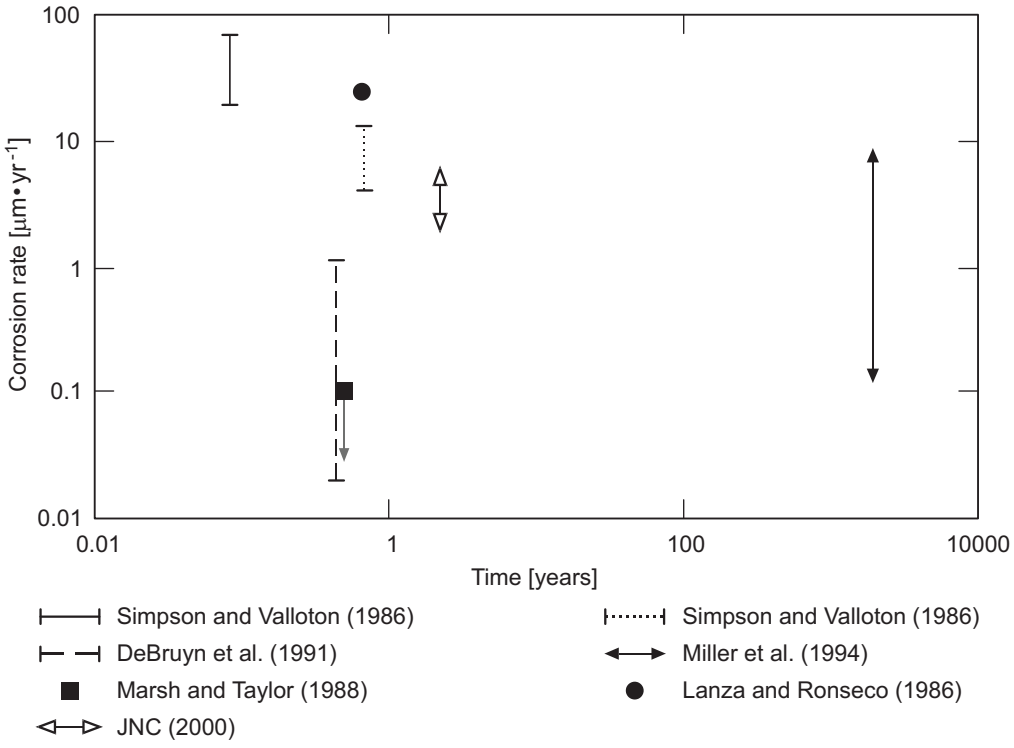

(b) Mass loss data

Figure 2: Compilation of anaerobic corrosion rates for carbon steel used in current Nagra canister lifetime prediction (Johnson and King 2003)

2.1 Results of experimental studies

2.1.1 Smart and co-workers, SKB

Smart and co-workers have performed a number of studies of the anaerobic corrosion of C-steel and cast iron for SKB (Peat et al. 2001; Smart et al. 2001, 2002a, b). Corrosion rates were measured by both weight-loss (periods up to 4 yrs) and from the rate of generation of H_2 (periods up to 1.4 yrs). Oxygen was rigorously excluded from the test environments, although the autoclaves containing the weight-loss specimens were initially air-filled and were opened in the lab atmosphere periodically as samples were removed for analysis. Experiments were performed in a number of simulated groundwater and bentonite pore-water solutions, with various over-pressures of H_2, at temperatures of 30 – 90 °C, and with and without pre-formed Fe_3O_4 or $FeCO_3$ surface films.

Figure 3 shows the time dependence of the corrosion rate of C-steel in a dilute Allard granitic groundwater at 90 °C measured by mass-loss over periods of up to 4 yrs. The composition of the groundwater is given in Table 1. The corrosion rates are the mean from six samples, although no indication of the variability of the rates was given. The observed corrosion rates are generally < 1 $\mu m \cdot yr^{-1}$ and exhibit a tendency to decrease with increasing exposure time, with observed time dependences between from $t^{-0.19}$ to $t^{-0.45}$. The exception to this trend of decreasing corrosion rate with time is the plain (non-welded) samples with a H_2 over-pressure of 1 MPa which shows an increase in rate after 4 yrs exposure (Figure 3(a)). Smart et al. (2001, 2002b) did not refer to this exception and, instead, used the general decrease in rate with time as evidence for the development of a protective corrosion product film.

Table 1: Composition of artificial groundwater solutions used by Smart et al. (2001; 2002a, b)

(Concentrations in mM)

Species	Allard	Äspö	Bentonite pore water	Solution for mass-loss tests
Na^+	2.84	131.3	560	6
K^+	0.10	0.19	0	–
Ca^{2+}	0.45	109.5	0	1.5
Mg^{2+}	0.18	2.06	0	1.26
Cl^-	1.96	339.6	540	3
Total carbonate	2.00	0.18	10	5.63
SO_4^{2-}	0.10	7.40	0	–
SiO_2	0.21	–	–	0.5
pH	8.1	7.0 to 8.0	10.5	9.4

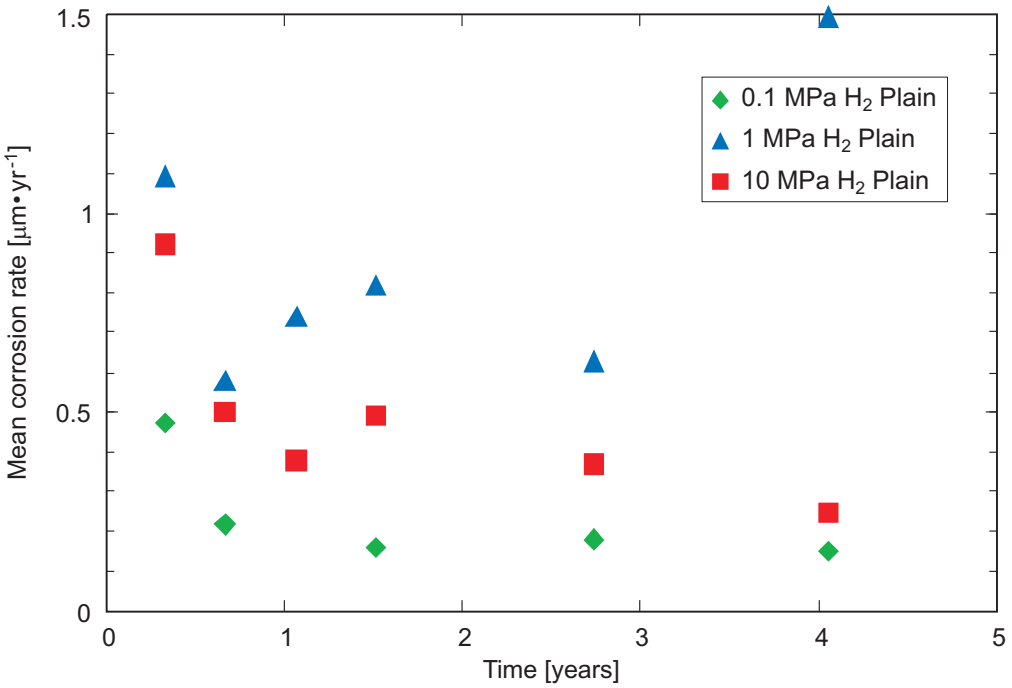

(a) Plain samples

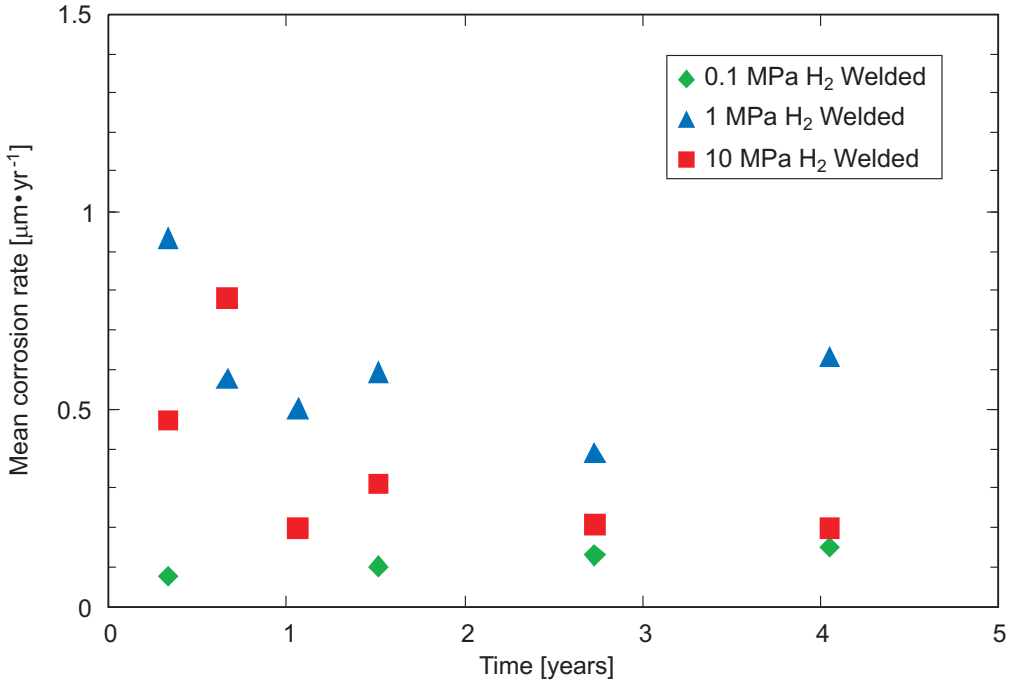

(b) Autogenous electron-beam welded samples

Figure 3: Time dependence of the mass-loss corrosion rate for carbon steel exposed to deaerated dilute granitic groundwater at 90 °C with various hydrogen over-pressures (Smart et al. 2001, 2002b)

There was no clear effect of the H_2 overpressure on the corrosion rate. The corrosion rates were consistently higher at the intermediate p_{H2} (1 MPa) for both plain and welded specimens, with the lowest rates observed at the lower pressure of 0.1 MPa. The authors concluded, however, that the variation in rate for different p_{H2} was within the experimental uncertainty and that, therefore, there is no effect of H_2 pressure on the corrosion rate.

There is no apparent difference between the corrosion rates for plain and welded specimens.

Specimens were observed to become covered by a black mottled corrosion product. Samples of the corrosion product were taken from 12-month specimens not used for mass-loss measurements and were found by XRD to consist of Fe_3O_4. In later studies, *ex situ* Raman spectroscopy was used to identify the nature of the corrosion products formed under similar exposure conditions (Rance et al. 2004). Both Fe_3O_4 and goethite (α-FeOOH) were identified, although it is possible that the latter formed upon exposure of the sample to air, as it was only observed on samples examined in a "wet" condition.

The tendency for the corrosion rate to decrease with exposure time was confirmed by the results of the H_2-evolution tests. Figure 1 shows an example of the results from these experiments, in which the rate of H_2 generation provides a more-instantaneous measure of the corrosion rate (averaged between measurements of the gas volume at a mean interval of ~ 300 hrs). Unlike the mass-loss tests, there was no evidence for an increase in corrosion rate at longer times in any of the 15 – 20 gas generation experiments. (The possible increase in corrosion rate described above was only observed after 4 yrs in the mass-loss tests, compared with maximum exposure times of 1.4 yrs in the gas-generation experiments). The authors did not calculate the time-dependence of the corrosion rates for comparison with the mass-loss data (and did not provide tabulated rates), but the figures seem to indicate a stronger tendency for the corrosion rates to decrease with time in the gas-generation tests. At longer times the corrosion rate appeared to reach a constant value, with rates of $< 0.1\ \mu m \cdot yr^{-1}$ (Figure 1).

Other conclusions from the gas-generation tests in groundwaters by Smart and co-workers include:

- in Allard groundwater (Table 1), the initial corrosion rate was higher at 50 ^oC than at 30 ^oC, although the long-term rate was about the same,
- pre-filming the samples with either $FeCO_3$ or Fe_3O_4 reduced the initial high corrosion rate, with thicker films more effective than thinner films and Fe_3O_4 more protective than $FeCO_3$ (no quantification of the terms "thick" and "thin" was provided by the authors),
- addition of Fe(II) to the solution (to aid the formation of the corrosion product film) had no effect on the corrosion rate,
- the corrosion rate was higher in high ionic strength groundwaters, with a threshold somewhere between the un-concentrated and 10-fold concentrated Allard groundwater, although this effect appears sub-ordinate to the decrease in corrosion rate with increasing pH,
- corrosion rates at 50 ^oC for cast iron were ~ 5 × lower than for C-steel, but at 85 ^oC the rates for the two materials were the same, and
- removing the non-adherent corrosion product using a tissue resulted in only a minor and temporary increase in corrosion rate.

These observations, and the results of other electrochemical experiments to be discussed below, lead the authors to propose that the corrosion rate is anodically controlled by ion transport across the inner barrier layer of a duplex Fe_3O_4 film on the surface. No direct evidence for the duplex nature of the film was provided, with indirect evidence only from the minimal effect on

the corrosion rate of removing loosely adherent corrosion product (see above). The authors suggest that corrosion occurs under active conditions and that the film retards the corrosion rate rather than passivating the surface. No evidence for localized corrosion was observed.

In later tests, Smart et al. (2004) measured the rate of H_2 production from C-steel and cast iron samples exposed to deaerated bentonite slurry at temperatures of 30 ^oC and 50 ^oC. The bentonite-water ratio was 0.3 with the simulated pore-water having a composition similar to that given for bentonite pore water in Table 1. Corrosion rates were slightly higher initially than those observed earlier in groundwater solutions, but the long-term rate after ~ 1.5 yrs was similar (≤ 1 $\mu m \cdot yr^{-1}$). Post-test Raman analysis identified mixtures of Fe_3O_4, Fe_2O_3, and α-FeOOH, although the latter Fe(III) species may have been due to residual O_2 in the test apparatus or post-sampling oxidation. Similar corrosion products were observed after exposure of C-steel to compacted bentonite in a similar environment (Carlson et al. 2006, Smart et al. 2008) and in tests involving a stack of alternating Cu and C-steel discs (Smart et al. 2006a).

The higher initial corrosion rate was explained by Fe(II) adsorption by the bentonite which retarded the formation of a protective corrosion product film. However, to explain the absence of an effect of added Fe(II) in their earlier work, Smart et al. (2001, 2002b) suggested that it was the inner Fe_3O_4 layer (grown by a solid-state electrochemical process) and not the outer precipitated layer that provided corrosion protection. Adsorption of Fe(II) by bentonite would be more likely to retard the formation of the outer precipitated layer rather than the inner solid-state grown film.

The same H_2 generation method was used to monitor the anaerobic corrosion rate of C-steel in compacted bentonite saturated with 1 $mol \cdot dm^{-3}$ NaCl (Smart et al. 2006b). Again, the corrosion rate was observed to decline with time, with rates of 1 – 3 $\mu m \cdot yr^{-1}$ observed after ~ 6 months exposure. It is interesting to note that the same workers using the same technique have consistently observed higher corrosion rates in the presence of bentonite (either compacted or as a slurry) than in bulk solution after similar exposure periods (1 – 3 $\mu m \cdot yr^{-1}$ in the presence of bentonite versus 0.5 – 1 $\mu m \cdot yr^{-1}$ in solution, Figure 1). This difference may reflect the retarding effect on film growth of Fe(II) adsorption by bentonite.

The corrosion rate measurements of Smart and co-workers appear to strongly and consistently support the suggestion that protective corrosion product films will develop on C-steel and cast iron under anaerobic conditions and that long-term corrosion rates will be of the order of 0.1 - 1 $\mu m \cdot yr^{-1}$.

The data produced by Smart and co-workers are considered to be reliable for the estimation of the long-term anaerobic corrosion rate, particularly those determined over exposure periods of several years. Care was exercised in the experimental procedures and the results are internally consistent.

2.1.2 Simpson, Schenk and Kreis, Switzerland

A number of relevant corrosion studies were performed as part of the Nagra's crystalline rock program in the 1980's (Kreis and Simpson 1992, Schenk 1988, Simpson 1984, Simpson and Valloton 1986, Simpson and Weber 1992, Simpson et al. 1985). As with the later work of Smart et al., Simpson and co-workers used a combination of mass-loss and H_2-generation measurements to determine the anaerobic corrosion rates of cast steel and nodular cast iron. Various natural and synthetic groundwaters, as well as NaCl solutions of different pH values (controlled by addition of HCO_3^-/CO_3^{2-}) were used at test temperatures of between 25 ^oC and 140 ^oC. The

compositions of the two groundwaters used (the natural Säckingen water and the synthetic Böttstein water) are given in Table 2. A limited number of tests were also performed with either compacted bentonite or a groundwater/bentonite slurry.

Table 2: Composition of artificial groundwater solutions used by Simpson et al. (1985) and Simpson (1984)

(Concentrations in mM)

Species	Säckingen water	Böttstein water
Na^+	43	209
K^+	2.1	1.4
Ca^{2+}	3.5	27
Mg^{2+}	0.56	0.12
Cl^-	46	228
F^-	0.13	0.20
HCO_3^-	4.8	
SO_4^{2-}	1.2	19
pH	6.5	

Unlike the closed system employed by Smart et al., the immersion tests performed in the Swiss programme were conducted using a continuously refreshed autoclave (for tests at > 100 ^oC) or vessel (at lower temperatures). A refreshed system was used to avoid the consumption of O_2 in those tests in which a constant dissolved O_2 concentration of 0.1 $\mu g \cdot g^{-1}$ was used (not reported here). The same apparatus was used for the nominally deaerated tests (estimated residual $[O_2]$ of ≤ 2 $\mu g \cdot g^{-1}$), but there is the danger with such open systems that O_2 could more-easily contaminate the test solution. Corrosion rates determined from the H_2-generation tests were, of course, estimated from the rate of H_2 generation (assuming the formation of Fe(II) only) and, unless the rate of H_2 generation is affected by the presence of any Fe(III) that might be formed by adventitious O_2, should be insensitive to possible O_2 contamination of the test cells.

As with the Smart et al. work discussed above, the measured corrosion rate decreased with increasing exposure time. This decrease is consistent with the formation of a protective corrosion film, although Kreis and Simpson (1992) suggest that the build-up of H_2 pressure might be responsible instead, even though the pressures involved are much lower than the equilibrium pressures for Fe corrosion as either $Fe(OH)_2$ or as Fe_3O_4 (see Section 3.1 for estimates of the equilibrium H_2 pressure). These authors concluded that limitation of the corrosion rate by film build up was unlikely because "the passive film is metastable with respect to an $Fe_{3-x}O_4$ phase." It is not clear what the authors meant by this since the nature of the corrosion film was not identified. Furthermore, the suggestion that increasing p_{H2} might suppress the rate of corrosion seems an unlikely cause of the observed decrease in corrosion rate since later tests by Smart et al. (2001; 2002a, b) have shown no effect of H_2 overpressure on either the corrosion or electrochemical behaviour of C-steel at pressures far in excess of those reported by Kreis and Simpson (1992).

Because of this effect of the exposure time on the measured corrosion rate, the data of Simpson and co-workers must be compared carefully with that of Smart et al. Typically, Simpson et al. performed H_2-generation experiments for a period of 8 – 16 days and reported a steady-state corrosion rate determined from the latter half of the test period. In the later study of Kreis and

Simpson (1992), however, there is evidence that the corrosion rate does not reach a steady state until ~ 4000 hrs (~ 6 months), a period that is more consistent with the observations of Smart et al. (2001, 2002b) shown in Figures 1 and 3. Some mass-loss immersion tests were conducted for periods up to 6300 hrs, although it is not possible to determine from the few measurements reported whether a steady-state had been achieved within this time period.

A limited number of immersion studies were performed with cast steel and nodular cast iron in the Säckingen and Böttstein waters at temperatures of 80 °C and 140 °C. Simpson et al. (1985) give anaerobic corrosion rates of 5 – 10 $\mu m \cdot yr^{-1}$ after an exposure period of 260 days at 80 °C, with no apparent difference between either the two materials or the two environments. No localized corrosion was observed. The degree of surface roughness was quantified for tests with 0.1 $\mu g \cdot g^{-1}$ O_2 (maximum peak height 5 μm after 260 days), although not apparently for the deaerated tests (Simpson 1984). It was later stated that the corrosion rate in Böttstein water is higher at 80 °C than at 140 °C (Simpson and Weber 1992), although the data presented for deaerated solution do not support this claim and it may only apply to measurements with 0.1 $\mu g \cdot g^{-1}$ O_2.

Corrosion rates were also determined in compacted bentonite at two densities corresponding to saturated moisture contents of 0.21 and 0.30 (clay dry densities of approximately 1.6 $Mg \cdot m^{-3}$ and 1.4 $Mg \cdot m^{-3}$, respectively). Corrosion rates for cast steel after 90 days were of the order of 8 – 12 $\mu m \cdot yr^{-1}$ for the higher density bentonite and 14 - 29 $\mu m \cdot yr^{-1}$ at the lower density (Simpson et al. 1985). In this case, the rates at 140 °C were consistently lower than those at 80 °C, although the significance of this trend is unclear as no experimental variability was given for the measured rates. However, in all the data presented for the two time periods reported, the rates were consistently higher for the lower bentonite density. No description or characterization of surface corrosion products from the immersion tests were provided.

The majority of corrosion rates reported were determined using the H_2-generation method (Schenk 1988, Simpson 1989). Table 3 shows a compilation of data given by Simpson (1989), but previously reported by Schenk (1988). The corrosion rates given are supposedly steady-state rates measured after 8 - 16 days exposure. In all cases the H_2-generation (corrosion) rate decreased with time.

Under near-neutral pH conditions (i.e., natural Säckingen and artificial Böttstein waters, and pH 7 Cl^- solutions), the corrosion rate reached a maximum value at a temperature of between 50 °C and 80 °C. This maximum may indicate a change in the protective nature of the corrosion products, possibly from $Fe(OH)_2$ to Fe_3O_4, although no characterization of corrosion products was reported. At higher pH (pH 8.5 or pH 10, Table 3), the corrosion rate tended to increase with temperature.

There is no apparent dependence of corrosion rate on Cl^- concentration, although the natural and synthetic groundwater solutions tended to give higher corrosion rates. (For comparison, the Cl^- content of Säckingen and Böttstein waters are ~ 1500 $\mu g \cdot g^{-1}$ and 8100 $\mu g \cdot g^{-1}$, respectively, Table 2). There is clearly an effect of increasing pH, as would be expected, with a trend towards passive behaviour, possibly enhanced by the presence of HCO_3^-/CO_3^{2-} to buffer the pH in the alkaline range.

In the original publication of these data, Schenk (1988) classified the various environments into five categories grouped according to the observed corrosion behaviour (Table 4). In all experiments, the H_2-generation rate exhibited an initial high rate indicative of active dissolution followed by a decrease, as typified by Schenk's Category B2 which he classified as "active becoming passive" behaviour. The environments that produced this behaviour were typically neutral/

near-neutral pH with low [Cl^-] (0 - 80 ppm) at moderate temperature (50 °C). Increasing the temperature to 80 °C resulted in higher quality protective layers (although the mean corrosion rate increases) (Category A1, Figure 4). The environments in Category A1 extend to higher [Cl^-] than Category B2 and include the two groundwater solutions. The same environments produced poorer-quality protective layers at temperatures of 25 °C and 50 °C, particularly at higher [Cl^-] (Category B1, Figure 4). Increasing the pH resulted either in passivity at pH 10 and correspondingly lower corrosion rates (Category C2) or marginal passivity and some evidence for localized corrosion at combinations of increased pH and/or increased [Cl^-].

Table 3: Compilation of anaerobic corrosion rates of cast steel measured using the hydrogen generation method (Simpson 1989)

Environment	**Temperature (°C)**	**Corrosion rate ($\mu m \cdot yr^{-1}$)**	**Category**
Säckingen	25	1.8	B1
Säckingen	50	3.6	B1
Säckingen	80	1.7	A1
Böttstein	25	1.3	B1
Böttstein	50	7.0	B1
Böttstein	80	2.7	A1
pH 7, 0 ppm Cl^-	50	2.8	B2
pH 7, 80 ppm Cl^-	50	3.0	B1
pH 7, 800 ppm Cl^-	50	1.4	B3
pH 7, 8000 ppm Cl^-	50	3.5	B3
pH 7, 0 ppm Cl^-	80	1.0	A1
pH 7, 80 ppm Cl^-	80	3.9	A1
pH 7, 800 ppm Cl^-	80	5.9	A1
pH 7, 8000 ppm Cl^-	80	0.8	A1
pH 8.5, 0 ppm Cl^-	50	0.8	B2
pH 8.5, 80 ppm Cl^-	50	0.8	B2
pH 8.5, 800 ppm Cl^-	50	1.4	B3
pH 8.5, 8000 ppm Cl^-	50	1.4	B1
pH 8.5, 0 ppm Cl^-	80	0.6	A1
pH 8.5, 80 ppm Cl^-	80	1.7	B3
pH 8.5, 800 ppm Cl^-	80	0.6	B3
pH 8.5, 8000 ppm Cl^-	80	2.8	B1
pH 10, 0 ppm Cl^-	50	< 0.04	C2
pH 10, 80 ppm Cl^-	50	< 0.04	C2
pH 10, 800 ppm Cl^-	50	< 0.04	C2
pH 10, 8000 ppm Cl^-	50	< 0.04	C2
pH 10, 0 ppm Cl^-	80	0.6	C2
pH 10, 80 ppm Cl^-	80	2.8	B3
pH 10, 800 ppm Cl^-	80	0.8	B3
pH 10, 8000 ppm Cl^-	80	0.6	C2

Table 4: Classification of anaerobic corrosion rates of cast steel based on observed corrosion behaviour (Schenk 1988)

Rates determined from hydrogen generation measurements. Errors given as +/– one standard deviation as estimated by the current author from the reported rates

Category	**Environment**	**Temperature (^{o}C)**	**Corrosion rate ($\mu m \cdot yr^{-1}$)**
A1 High-quality protective film Mean corrosion rate 2.4 ± 2.0 $\mu m \cdot yr^{-1}$	Säckingen	80	1.7
	Böttstein	80	2.7
	pH 7, 0 ppm Cl^-	80	1.0
	pH 7, 80 ppm Cl^-	80	3.9
	pH 7, 800 ppm Cl^-	80	5.9
	pH 7, 8000 ppm Cl^-	80	0.8
	pH 8.5, 0 ppm Cl^-	80	0.6
B1 Low-quality protective layer Mean corrosion rate 3.0 ± 2.0 $\mu m \cdot yr^{-1}$	Säckingen	25	1.8
	Säckingen	50	3.6
	Böttstein	25	1.3
	Böttstein	50	7.0
	pH 7, 80 ppm Cl^-	50	3.0
	pH 8.5, 8000 ppm Cl^-	50	1.4
	pH 8.5, 8000 ppm Cl^-	80	2.8
B2 Passive after initial active phase Mean corrosion rate 1.5 ± 1.2 $\mu m \cdot yr^{-1}$	pH 7, 0 ppm Cl^-	50	2.8
	pH 8.5, 0 ppm Cl^-	50	0.8
	pH 8.5, 80 ppm Cl^-	50	0.8
B3 "Unstable passivity," localized attack Mean corrosion rate 1.8 $\mu m \cdot yr^{-1}$ plus transients	pH 7, 800 ppm Cl^-	50	1.4
	pH 7, 8000 ppm Cl^-	50	3.5
	pH 8.5, 800 ppm Cl^-	50	1.4
	pH 8.5, 80 ppm Cl^-	80	1.7* (1.0)
	pH 8.5, 800 ppm Cl^-	80	0.6
	pH 10, 80 ppm Cl^-	80	2.8* (1.6)
	pH 10, 800 ppm Cl^-	80	0.8* (6.0)
C2 Passive Mean corrosion rate 0.2 ± 0.3 $\mu m \cdot yr^{-1}$	pH 10, 0 ppm Cl^-	50	< 0.04
	pH 10, 80 ppm Cl^-	50	< 0.04
	pH 10, 800 ppm Cl^-	50	< 0.04
	pH 10, 8000 ppm Cl^-	50	< 0.04
	pH 10, 0 ppm Cl^-	80	0.6
	pH 10, 8000 ppm Cl^-	80	0.6

* Denotes discrepancy between corrosion rates given by Simpson (1989) and the original work of Schenk (1988) given in parentheses

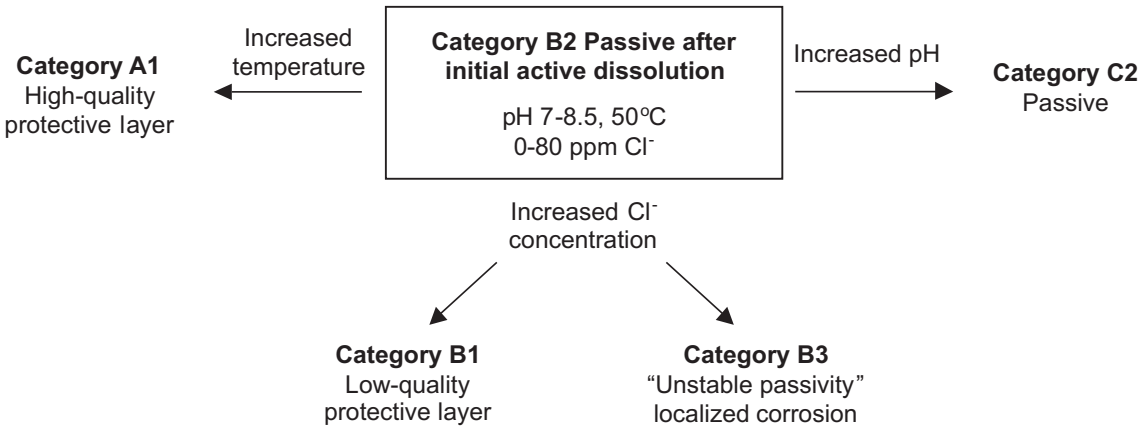

Figure 4: Categorization of corrosion behaviour of cast steel in groundwater and chloride environments (Schenk 1988)

It is apparent from these results that a variety of behaviour is observed, depending on the pH, Cl^- content, and temperature. Given that the canister surface temperature will be greater than 80 °C for the first 500 - 900 yrs (Nagra 2002) and that the bentonite pore water pH will be buffered ~ pH 7 - 8, it seems likely that, based on this classification, a steel canister in an Opalinus Clay repository would most likely corrode with the formation of a protective layer (Categories A1 or B1).

Although localized corrosion was reported, Schenk (1988) and Simpson (1989) do not comment on the mechanism and whether anodic and cathodic sites are permanently separated.

Based on the assumption that the canister will form a protective film, the data in Tables 3 and 4 suggest a mean corrosion rate of 1 – 3 $\mu m \cdot yr^{-1}$ based on short-term H_2-generation rates (exposure period of 8 – 16 days). However, the longer-term studies reported by Kreis and Simpson (1992) imply that significantly lower corrosion rates can be expected at longer times (Figure 5). Table 5 shows the time dependence of the corrosion rate in three different environments, highlighting the fact that the rate continues to decrease for several thousand hours and that the short-term rates reported by Schenk (1988) and Simpson (1989) are likely to have been far from steady state. In fact, Kreis and Simpson's (1992) data suggests that steady state is only achieved after ~ 6 months exposure. The short-term rates in Figure 5 are similar to those reported at the same temperature by Schenk (1988) and Simpson (1989). Based on the longer-term rates, a better estimate of the anaerobic corrosion rate of cast steel in these environments is of the order of 0.1 $\mu m \cdot yr^{-1}$. Given the long-term nature of the experiments, this rate is considered to be a reliable estimate of the long-term anaerobic corrosion rate of C–steel.

Table 5: Anaerobic corrosion rates of cast steel determined from long-term hydrogen generation tests at 25 °C (Kreis and Simpson 1992)

(Corrosion rates in $\mu m\ yr^{-1}$)

Exposure time (Hrs)	8000 ppm Cl^-, pH 8.5	Böttstein water	Double-distilled water
200	0.5*	0.5	0.5
2000	0.1	0.1	0.1
7500	0.06	0.04	0.04

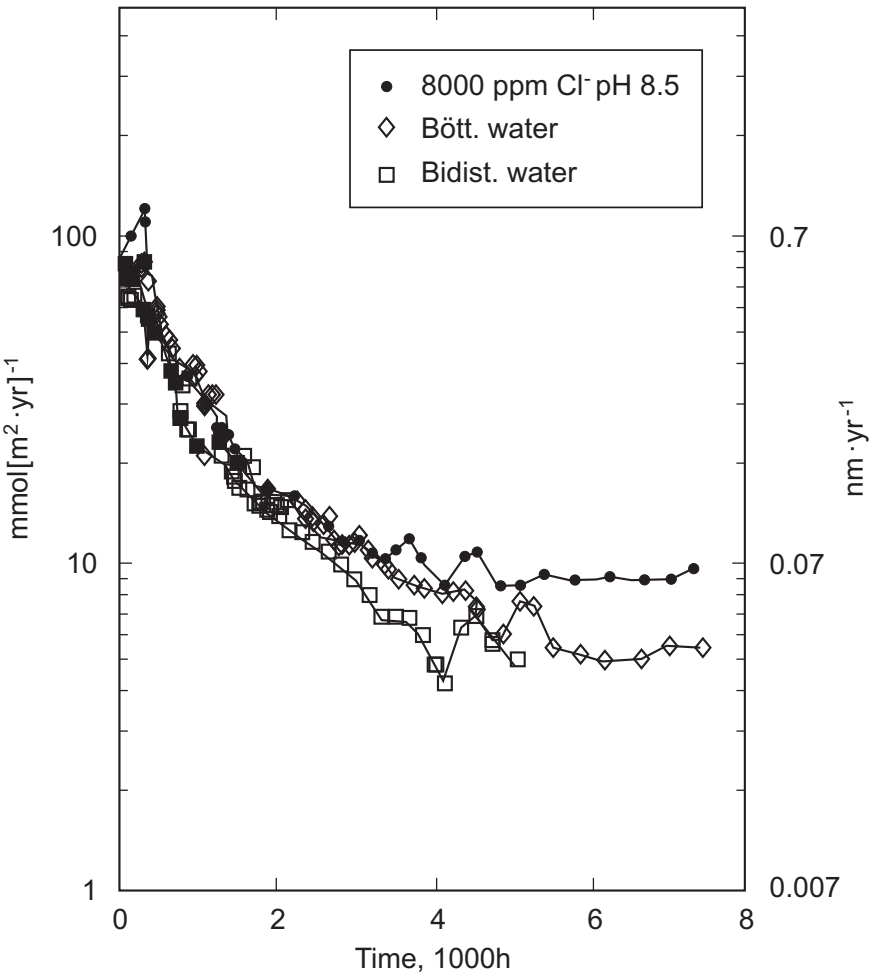

Figure 5: Hydrogen generation rates for cast steel in near-neutral pH environments at 25 °C reported by Kreis and Simpson (1992)

Note: The corrosion rate scale is in μm yr^{-1}, not nm/yr as stated

2.1.3 Japanese studies

JNC (2000) published a compilation of anaerobic corrosion rates for C-steel as part of the H–12 project (Figure 6). Most of the Japanese corrosion rates are time-averaged rates measured using the mass-loss technique, although a small number of short-term H_2-generation experiments were also carried out in synthetic seawater at 80 °C. The data covered a maximum exposure period of 4 yrs, with plans supposedly to extend the tests up to 10 yrs (Taniguchi et al. 2004). To date, none of these very long-term measurements have been published.

In common with all other studies, the data in Figure 6 show a strong tendency of decreasing corrosion rate with increasing exposure period. The data come from a number of sources and from both mass-loss and H_2-generation measurements in both bulk solution and in compacted bentonite. Perhaps as a consequence, there is considerable scatter in some of the data, especially for periods ≤ 1 yr. It is interesting to note that for these shorter-term tests, the lowest corrosion rates were measured using the H_2-generation technique (which gives "instantaneous" rates) or by mass-loss in closed systems (which tend not to suffer from O_2 ingress in the same way as recirculating systems).

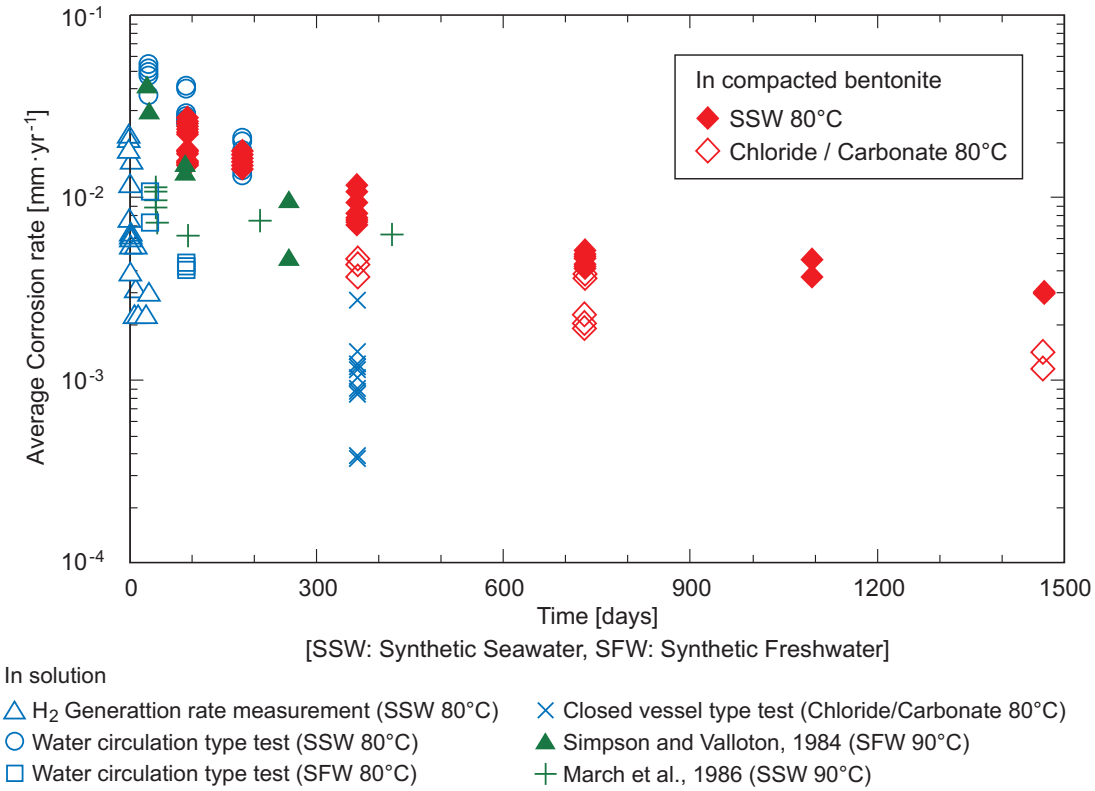

Figure 6: Long-term anaerobic corrosion rates for carbon steel in solution and compacted bentonite at a temperature of 80 – 90 °C (JNC 2000); majority of rates measured from mass-loss with some H_2-generation data also shown

Table 6: Composition of test solutions used by Taniguchi et al. (2004)

(Concentrations in mM)

Species	**Synthetic seawater (SSW)**	**Synthetic groundwater – 1 (SGW-1)**	**Synthetic groundwater – 2 (SGW-2)**
Cl^-	560	560	2.5
SO_4^{2-}	29		
HCO_3^-	2.4	100	2.5
F^-	0.07		
Br^-	0.86		
BO_3^{3-}	0.44		
Na^+	480	660	5
K^+	10		
Ca^{2+}	10		
Mg^{2+}	55		
Sr^{2+}	0.7		
pH	7.9 – 8.4	8.3 – 8.7	9.1 – 9.2

The longest tests were those in compacted bentonite which are discussed in some detail by Taniguchi et al. (2004). Triplicate coupons of a rolled and a forged C–steel (plain or electron-beam welded) were exposed to compacted buffer material (either 100 % bentonite, ρ_d 1.8 $Mg \cdot m^{-3}$; or 70 : 30 bentonite : sand, 1.6 $Mg \cdot m^{-3}$) saturated with either deaerated synthetic seawater or one of two synthetic groundwater solutions (Table 6) and exposed at temperatures of 50 °C or 80 °C. The dry clay mixtures were pre-compacted and then evacuated and flushed with N_2 gas before saturating with the deaerated solution. Post-test analysis of corrosion products was performed by SEM, XRD, and EPMA for elemental analyses. Samples were transferred to the analytical instruments without (or with minimal) air exposure. A total of seven test conditions were reported by Taniguchi et al. (2004) (Table 7). Because of the efforts to exclude O_2 from the tests, it appears that the tests were conducted under rigorous anaerobic conditions.

Table 7: Test conditions reported by Taniguchi et al. (2004)

Estimated from the slope of the mass loss as a function of time*

No.	Solution	Temperature (°C)	Test period(s) (yrs)	Sample type	Buffer material	Corrosion rate after 1 yr* ($\mu m \cdot yr^{-1}$)	Corrosion rate after 3 - 4 yrs * ($\mu m \cdot yr^{-1}$)
1	SSW	80	0.25, 0.5, 1, 2, 3, 4	Rolled	100 % bentonite	7.0	0.99
2	SSW	50	1, 2, 3	Rolled	100 % bentonite	4.0	1.9
3	SGW-1	80	1, 2, 3, 4	Rolled	100 % bentonite	4.2	0.18
4	SGW-2	80	1, 2, 3	Rolled	100 % bentonite	7.4	0.62
5	SSW	80	1	Rolled	70 : 30 bentonite : sand	–	–
6	SSW	80	1, 2, 3	Forged	70 : 30 bentonite : sand	18	0.54
7	SSW	80	1, 3	Forged, welded	70 : 30 bentonite : sand	18	0.76

Samples were removed at the end of the test periods noted in Table 7. Corrosion was uniform in nature and no localized corrosion was observed. The samples exposed at 80 °C were covered by an adherent black corrosion product, whereas the black corrosion product on samples exposed at 50 °C was poorly adhered. The corrosion products formed at 80 °C were identified by XRD as $FeCO_3$ and, in some cases, $Fe_2(OH)_2CO_3$, but no Fe_3O_4 was found. Elemental compositions were consistent with the XRD data, except for the presence of Ca^{2+} in all samples, even those exposed to SGW-1 and SGW-2 solutions which did not contain Ca^{2+} (although calcite is likely present as a mineral impurity in the bentonite). The presence of carbonate corrosion products on samples in contact with compacted bentonite, rather than oxides, is consistent with findings from similar Japanese and French studies (Dong et al. 2001, Papillon et al. 2003, Tsushima et al. 2003). The thickness of the corrosion products was less than that which would be predicted based on the sample mass loss and suitable volume expansion, indicating that a significant portion of the dissolved Fe(II) had diffused into the compacted bentonite, consistent with the observations of Smart et al. (2006b, 2008).

A further point to note in the various studies of corrosion in compacted bentonite is that the rates do not seem to differ significantly for different bentonites (cf. Table 7 for Japanese Kunigel bentonite and Figure 1b for MX-80 bentonite).

As in other studies, the corrosion rate was found to decrease significantly with increasing time of exposure (Figure 7). After an exposure period of 3 years, mass-loss corrosion rates were reported to be in the range 1.2 to 6.8 $\mu m \cdot yr^{-1}$. Higher corrosion rates were observed with the SSW-saturated bentonite, for a reason that was unknown. In addition, higher rates were observed in the lower density 70 : 30 bentonite : sand mixture, possibly because of the higher rate of mass transport of dissolved Fe(II) away from the corroding surface and the consequent retardation of the growth of a protective $FeCO_3$ film. However, if adsorption of Fe(II) occurs, then one might expect higher corrosion rates in the 100 % bentonite as adsorption tends to lower the interfacial dissolved metal ion concentration and drive corrosion, as reported for copper in contact with compacted buffer material (King et al. 1992).

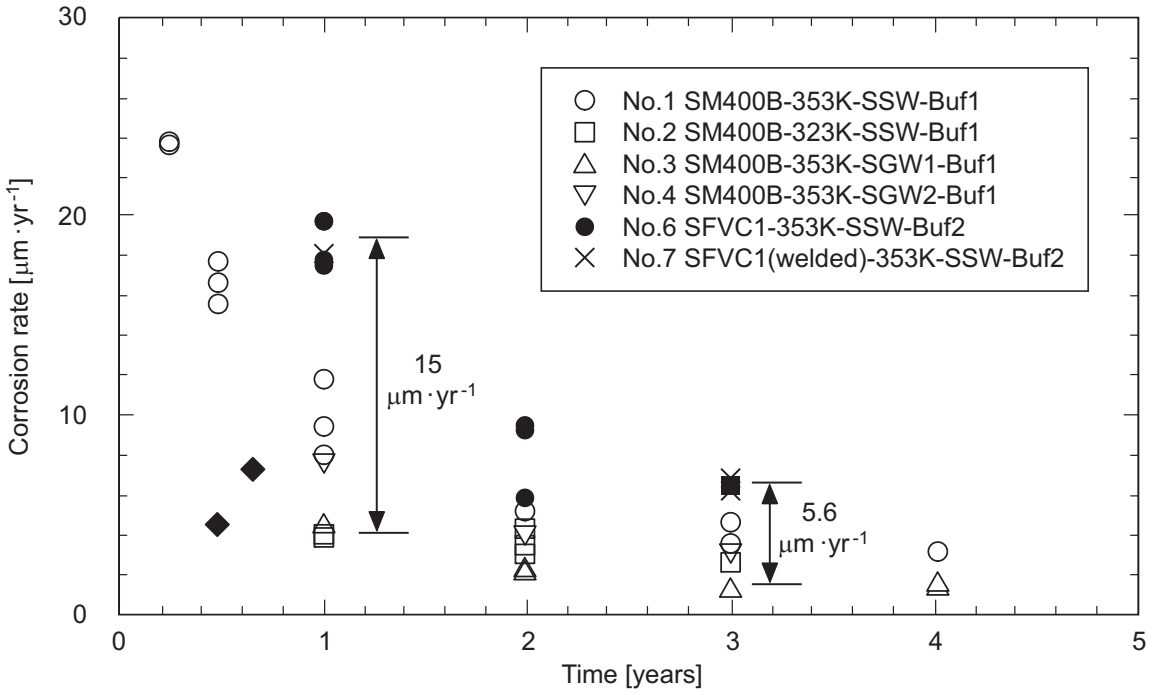

Figure 7: Observed time dependence of the anaerobic mass-loss corrosion rate of carbon steel in contact with compacted bentonite (Taniguchi et al. 2004); the two solid diamonds (♦) are mass-loss corrosion rates in compacted FoCa clay from Papillon et al. (2003)

Taniguchi et al. (2004) attempted to derive "instantaneous" corrosion rates by estimating the rate of mass loss from the time-dependent mass-loss data. Their estimated rates after 3 or 4 yrs exposure are given in the right-hand column of Table 7, along with estimates for an exposure period of 1 year. Based on this analysis, Taniguchi et al. (2004) concluded that the anaerobic corrosion rate of C–steel in compacted bentonite was ≤ 1 $\mu m \cdot yr^{-1}$ at 80 °C, with a rate of 2 $\mu m \cdot yr^{-1}$ at 50 °C (presumably as a consequence of a less-protective film at the lower temperature).

"Instantaneous" corrosion rates can also be estimated if the time dependence of the mass-loss rate is known. If the mass-loss increases with time (t) according to t^n then the instantaneous rate at a given time is n times the mass-loss rate determined over the same interval. For example, for parabolic film growth (n = 0.5), the instantaneous rate is ½ of the mass-loss rate. Thus, converting the time-averaged mass-loss rates in Figure 7 to instantaneous rates would give rates of 1 – 2 $\mu m \cdot yr^{-1}$ after 4-years exposure, consistent with the analysis of Taniguchi et al. (2004).

The Japanese work was carefully conducted and the corrosion rates are considered to be reliable. In particular, the rates derived from long-term experiments are considered to be suitable for estimating the anaerobic corrosion rate of C-steel canisters.

2.1.4 Marsh, Taylor and co-workers, UK

A number of studies of the corrosion behaviour of C-steel were performed in support of the U.K. program in the 1980's. Many of these measurements were made under aerobic conditions and are not discussed here, but Marsh and co-workers do refer to individual mass-loss measurements under anaerobic conditions which are summarized in Table 8.

Table 8: Compilation of anaerobic corrosion rates of carbon steel determined as part of the 1980's U.K. Program

Time-averaged rates measured using the mass-loss technique

Material	Environment	Exposure period (hrs)	Corrosion rate ($\mu m \cdot yr^{-1}$)	Reference
0.2 % C forged steel	Ar-purged synthetic granitic water, 450 $\mu g \cdot g^{-1}$ TDS, pH 9.4, 90 ^oC	5,000	< 0.1	Marsh and Taylor 1988
0.2 % C forged steel	Ar-purged synthetic seawater, 90 ^oC	10,000	~ 6	Marsh and Taylor 1988, Marsh et al. 1989
Cast steel	Ar-purged ASTM substitute seawater, 90 ^oC	5,000	8	Marsh et al. 1983

The anaerobic corrosion rates reported covered a wide range from < 0.1 $\mu m \cdot yr^{-1}$ to 6 – 8 $\mu m \cdot yr^{-1}$ with the higher rates observed in synthetic seawater environments. Relatively few experimental details or results of post-test analyses are provided, with the exception of the suggestion that a Fe_3O_4 film was formed on coupons exposed to a synthetic granitic groundwater-bentonite paste at 90 ^oC (Marsh and Taylor 1988).

Compared with the other studies discussed above, there are relatively few anaerobic corrosion rates reported in the early U.K. program. Furthermore, the rates reported exhibit some variability, which cannot be completely explained by the variability in the experimental conditions.

2.1.5 Miscellaneous nuclear waste management studies

Various other national programs that have considered the use of C-steel canisters have published studies of the anaerobic corrosion rate (Table 9). Papillon et al. (2003) studied the anaerobic corrosion of C-steel in compacted FoCa smectitic clay in support of the French program.

Five steel samples were exposed for periods of 6 months and 8 months at temperatures of 25 °C and 80 °C, respectively, to an anaerobic clay environment saturated with a dilute Na^+/HCO_3^--based groundwater. Prior to saturation, the clay (dry density 1.3 $Mg \cdot m^{-3}$) was repeatedly evacuated and flushed with Ar to remove atmospheric O_2. Gras (1996) and Crusset et al. (2001) analysed a wide range of literature corrosion rates and found a parabolic decrease in rate with time, attributed to the formation of a protective Fe_3O_4 film. Dridi (2005) studied the corrosion of C-steel in argillaceous environments and also found the corrosion rate decreased with time with approximately parabolic kinetics.

Table 9: Summary of other nuclear waste management studies of the anaerobic corrosion of steel

Time-averaged rates measured using the mass-loss technique

Material	Environment	Exposure period (hrs)	Corrosion rate ($\mu m \cdot yr^{-1}$)	Reference
1035 C-steel	Compacted FoCa clay (ρ_d 1.3 $Mg \cdot m^{-3}$), saturated with deaerated Na/HCO_3-based groundwater, 530 $\mu g \cdot g^{-1}$ TDS, pH 8.0, 25 °C	4,400 (6 months)	4 – 5	Papillon et al. (2003)
1035 C-steel	Compacted FoCa clay (ρ_d 1.3 $Mg \cdot m^{-3}$), saturated with deaerated Na/HCO_3-based groundwater, 530 $\mu g \cdot g^{-1}$ TDS, pH 8.0, 80 °C	5,800 (8 months)	7 – 8 + pitting	Papillon et al. (2003)
C-steel (as received)	Synthetic interstitial Boom clay water, 170 °C,	4,400 (6 months)	1.3	De Bruyn et al. (1991)
C-steel (undefined heat treatment)	Synthetic interstitial Boom clay water, 170 °C,	4,400 (6 months)	0.7	De Bruyn et al. (1991)
C-steel (welded)	Synthetic interstitial Boom clay water, 170 °C,	4,400 (6 months)	1.6	De Bruyn et al. (1991)
C-steel	*In situ* test in direct contact with Boom clay, possibly some initial trapped air, 16 °C	57 months	1.8	Kursten et al. (1996)
C-steel	*In situ* test in direct contact with Boom clay, possibly some initial trapped air, 90 °C	21 months	7.7	Kursten et al. (1996)
C-steel	*In situ* test in direct contact with Boom clay, possibly some initial trapped air, 90 °C	84 months	4.7	Kursten et al. (1996)
C-steel	*In situ* test in direct contact with Boom clay, possibly some initial trapped air, 170 °C	57 months	8.6	Kursten et al. (1996)

Measured mass-loss corrosion rates ranged from 4 – 5 μm·yr^{-1} at 25 ^{o}C and 7 – 8 μm·yr^{-1} at 80 ^{o}C (Table 9). These rates are consistent with the short-term rates observed by Taniguchi et al (2004) (Figure 7). Localized corrosion was also observed at the higher temperature in the form of hemi-spherical pits (maximum depth 50 μm) over the entire surface of the coupons. The authors discounted any possible role of residual O_2 or microbial activity, and instead suggested that Fe(III) released from the Fe-rich clay was responsible for the localized corrosion. The bentonite clay under consideration in Switzerland and other countries has a lower Fe content, consistent with the absence of any indications of localized corrosion in compacted clay systems. Another possible source of Fe(III) is crystalline goethite (on the scale of 10 – 100's nm) in the clay, although the authors suggested that this was reduced chemically by the H_2 generated by corrosion, which would not induce localized corrosion, rather than electrochemically by galvanic coupling to the steel surface, which could.

Alteration of the clay layer near the steel-clay interface was observed, especially at the higher temperature. At 25 ^{o}C, "nanometric" crystallites (presumably 10 – 100's nm in dimension) were observed at the steel/clay interface. These oxide particles were assumed to comprise Fe_3O_4, possibly formed from Fe(II) produced by the dissolution of the goethite microcrystals which were found to have preferentially dissolved within 100 μm of the steel surface. At 80 ^{o}C, calcite precipitation, as well as a mixed zone of calcite, $FeCO_3$, and an Fe(II)-altered clay (similar to berthierine) were observed.

Lanza and Ronsecco (1986) report a study of the corrosion of C-steel in compacted Boom clay and sea sediments at temperatures of 30, 50, and 90 ^{o}C for periods up to 220 days. The system was sealed and, although initially aerated, the authors suggested that considerable consumption of O_2 would have occurred during the course of the test. The time dependence of the observed mass loss was divided into an initial period and a later steady-state phase, the latter presumed to correspond to anaerobic conditions. "Anaerobic" corrosion rates could, therefore, be derived from the results and the data for Boom clay are plotted in Figure 2(b). However, because of uncertainties over the evolution of redox conditions within the test vessel and because of the possibility of accelerated corrosion supported by the reduction of Fe(III) species produced during the aerobic phase, these values are not considered as reliable a measure of the anaerobic corrosion rate as those from the other studies discussed above.

Carbon steel has been a candidate canister material in the Belgian program for a number of years and has been considered in a number of different repository designs. Corrosion studies have been performed in the laboratory and *in situ* in an underground research laboratory (Table 9). In laboratory testing, mass-loss corrosion rates of < 2 μm·yr^{-1} were observed for various C-steel coupons exposed to deaerated interstitial water at a temperature of 170 ^{o}C (De Bruyn et al. 1991, Kursten and Van Iseghem 1999, Kursten et al. 1996). (Interstitial water in equilibrium with Boom clay under aerobic conditions consists of a Mg-Na dominated sulphate solution with a total dissolved solids content of ~ 39 g/L. Oxidation of pyrite impurities leads to acidic waters. Under anaerobic conditions, limited oxidation occurs and interstitial waters will be less aggressive. It is unclear whether the interstitial water used in the lab studies under anaerobic conditions was itself prepared anaerobically or exposed to the laboratory atmosphere). Post-test surface analysis by optical and electron microscopy indicated a black crystalline corrosion product, confirmed by XRD to be Fe_3O_4.

Long-term corrosion tests performed *in situ* with coupons (probes) inserted in direct contact with the Boom clay produced mass-loss corrosion rates in the range 2 – 9 μm·yr^{-1}. The corrosion rate increased with increasing temperature, but decreased with increasing exposure time. Although some air would have been entrained upon emplacement of the samples, anaerobic conditions can be expected to have developed by the end of the test as a consequence of O_2

consumption by corrosion and by oxidation of pyrite impurities in the clay. However, the extent to which the initial aerobic phase contributed to the overall extent of corrosion in these tests is unknown, and the measured rates are not considered useful for the current review.

Gas production and transport is also of concern in L&ILW repositories. Bracke et al. (2004) reviewed a number of studies of the corrosion and gas generation "of iron in brine" (although the references were not cited) and developed the following expression for the dependence of the gas generation rate (R) on pH:

$$R = 3 \times 10^{7}\, e^{-2.08pH}\ dm^3 \cdot m^{-2} \cdot yr^{-1} \quad (1)$$

For Fe corroding anaerobically as Fe(II), this expression is equivalent to corrosion rates of 4.5 $\mu m \cdot yr^{-1}$ at pH 7, 0.56 $\mu m \cdot yr^{-1}$ at pH 8, and 0.07 $\mu m \cdot yr^{-1}$ at pH 9. Unfortunately, Bracke et al. (2004) provide few other details with which to determine the robustness of this expression.

A large number of other studies have been excluded from this review, either because they were conducted under aerobic conditions or in environments not considered relevant to the Nagra program, such as the studies in salt formations (e.g., Smailos et al. 1985, Westerman et al. 1986).

2.1.6 Non-nuclear waste management literature

Perhaps surprisingly, the non-nuclear waste management literature contains few useful studies of the corrosion of C-steel under anaerobic conditions. Carbon steel is used in a number of applications in anaerobic aqueous environments, but none provide relevant corrosion rate data (e.g., high-temperature water in boiler systems, anaerobic soils for underground pipelines, deep seawater applications). In soils and seawater there is inevitably some microbial contribution to the corrosion mechanism, whereas such activity is believed to be limited for canisters surrounded by compacted bentonite.

Platts et al. (1994) summarize the results from three studies of H_2 generation from the corrosion of Fe in pure water at temperatures between 25 ^{o}C and 100 ^{o}C. In relatively short-term tests (maximum 76 days), the equivalent corrosion rates were 0.7 – 1.2 $\mu m \cdot yr^{-1}$ (Gould and Evans 1947, Jelenik and Neufeld 1982, Seo et al 1987). The rate was apparently insensitive to temperature within this range.

2.1.7 Comparison of the anaerobic corrosion of carbon steel in bulk solution and compacted bentonite

Based on the results presented above, a number of differences between the corrosion behaviour of C-steel in bulk solution and in compacted bentonite are apparent (Figure 8). In bulk solution, an apparent steady-state corrosion rate is established after 4 – 6 months exposure, with a long-term ("instantaneous") rate of ~ 0.1 $\mu m \cdot yr^{-1}$ (Kreis and Simpson 1992, Smart et al. 2001). The decrease in corrosion rate with time is due to the formation of a duplex film comprising an inner epitaxially grown layer with a spinel-type structure and an outer Fe_3O_4 layer grown via a dissolution-precipitation mechanism.

	Bulk solution	Compacted bentonite
Corrosion rate and time dependence	~0.1 μm ·yr^{-1} Steady-state after 4-6 months e.g., Smart et al. (2001), Kreis and Simpson (1992)	~1 μm ·yr^{-1} Still decreasing after 4 yrs e.g., Taniguchi et al. (2004), Papillon et al. (2003)
Corrosion products: composition and structure	Duplex spinel-type/Fe_3O_4 structure 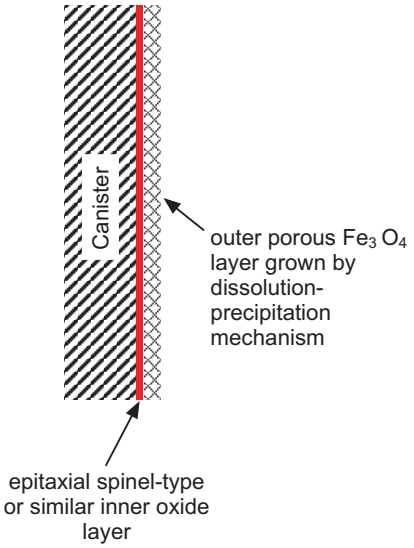	Thick $FeCO_3$/(Fe, Ca) CO_3-containing dense product layer and adjoining altered soil layer 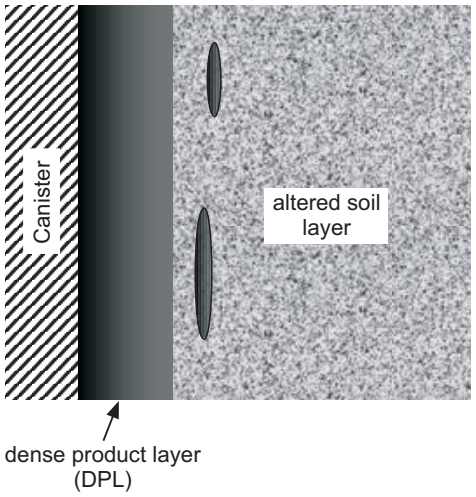

Figure 8: Comparison of anaerobic corrosion behaviour of carbon steel in bulk solution and in compacted bentonite

In compacted bentonite, the corrosion rate also decreases with increasing time of exposure, but steady state is not achieved after 4 yrs, at which time the corrosion rate is of the order of 1 μm·yr^{-1} (Taniguchi et al. 2004). Thicker corrosion product layers are typically observed at the steel-bentonite interface, with evidence for Fe and Ca carbonates (Papillon et al. 2003), although thinner corrosion product layers have also been reported (Carlson et al. 2006, Smart et al. 2008). The observation of thin corrosion product layers in the presence of bentonite suggests that sorption and transport of Fe(II) in the clay layer prevents the formation of thick precipitated layers.

2.1.8 Reliability of corrosion rates

The literature contains a large number of studies of the anaerobic corrosion rate of C-steel and cast iron, carried out under an equally large number of environmental conditions. The following criteria have been applied here in selecting those studies considered to be reliable sources for estimating the long-term anaerobic corrosion rate of C-steel canisters:

- long-term studies with exposure periods greater than 6 months,
- relevant bulk solution or compacted clay environments,
- internally consistent data sets and demonstrated time-dependent behaviour, and
- careful experimental technique, particularly in the exclusion of O_2.

2.2 Evidence from archaeological artifacts

The advantages offered by the use of archaeological artifacts are obvious. Many iron-based objects can be found that have been exposed to corrosive environments for many hundreds and thousands of years. The fact that these objects still exist is an indication that iron (and steel) does corrode slowly under certain environmental conditions. The problem of course is knowing exactly what these environmental conditions were during the course of the exposure period, particularly the redox conditions. Most artifacts are recovered from near-surface aerobic environments. Given that these conditions (apart, possibly, from the exposure temperature) are more corrosive than those during the anaerobic phase in the repository, the rates inferred from such artifacts can be considered to be conservative over-estimates of those for the canister. (This claim is based on the argument that aerobic, near-neutral conditions are unlikely to induce passivity of iron and steel in near-surface, near-neutral pH environments).

Both the French and Japanese nuclear waste management programs are investing a lot of effort in the study of archaeological artifacts. The French program uses evidence from artifacts to affirm the long-term corrosion mechanism(s), whereas the Japanese program is also using these studies to provide estimates of long-term corrosion rates.

Neff et al. (2006) outline a procedure for estimating corrosion rates from archaeological artifacts and report the results of measurements on ~ 40 objects from five different sites. The minimum corrosion rate was estimated from the amount of precipitated corrosion products by dividing the thickness of the corrosion product layer by the exposure period and a correction factor to account for the difference in density between the underlying metal and corrosion product. The maximum corrosion rate is estimated by adding an amount to account for the advective-diffusive loss of soluble corrosion products estimated by multiplying a fraction of the annual precipitation at the site by the solubility of the corrosion product.

Figure 9 shows a comparison of the rates estimated by Neff et al. (open symbols) with corrosion rates in soil taken from the literature (Neff et al. 2006). As with other studies described above, the selected rates exhibit a tendency to decrease with time. The rates inferred by Neff et al. (2006), which reflect a range of environmental conditions, are < 4 $\mu m \cdot yr^{-1}$.

Even lower corrosion rates are reported by Yoshikawa et al. (2007) from a study of ~ 1000 artifacts from a 1500-year-old site in Japan. The authors used an X-ray computer tomography technique to non-destructively map density differences in encrusted corrosion products, from which the location of the metal/oxide interface was estimated and a depth of corrosion inferred. Figure 10 shows a comparison of the results from these analyses with those extrapolated from relatively short-term experimental measurements. The rates inferred from the archaeological artifacts were in the range 0.1 to 1.1 $\mu m \cdot yr^{-1}$. Corrosion products observed included goethite (α-FeOOH), magnetite, lepidocrocite (γ-FeOOH), and akaganeite (β-FeOOH).

Crossland (2005, 2006) reviewed evidence for the long-term corrosion of iron and copper, including that from archaeological artifacts. Figure 11 shows the time-dependence of the depth of corrosion for iron and steel exposed to both soils and natural waters (fresh water, seawater, and ground waters). There is a spread of 2 – 3 orders of magnitude in the corrosion rate at a given time. Crossland (2005, 2006) somewhat arbitrarily attempted to delineate rates determined under aerobic conditions from those in anaerobic environments. Regardless of the lack of scientific evidence to support this distinction, it is apparent that there are a number of measurements with estimated corrosion rates of < 1 $\mu m \cdot yr^{-1}$.

In summary, the study of artifacts provides estimates of long-term corrosion rates under conditions that are difficult to easily relate to those to which a canister will be exposed. However, apart from the lower temperature, these conditions are likely to be more corrosive than those in a repository and, therefore, the inferred rates are conservative estimates for the canister. Given this, perhaps the most useful finding from the study of archaeological artifacts is that there are many instances in which iron and steel has been found to corrode at rates < 1 μm·yr^{-1}.

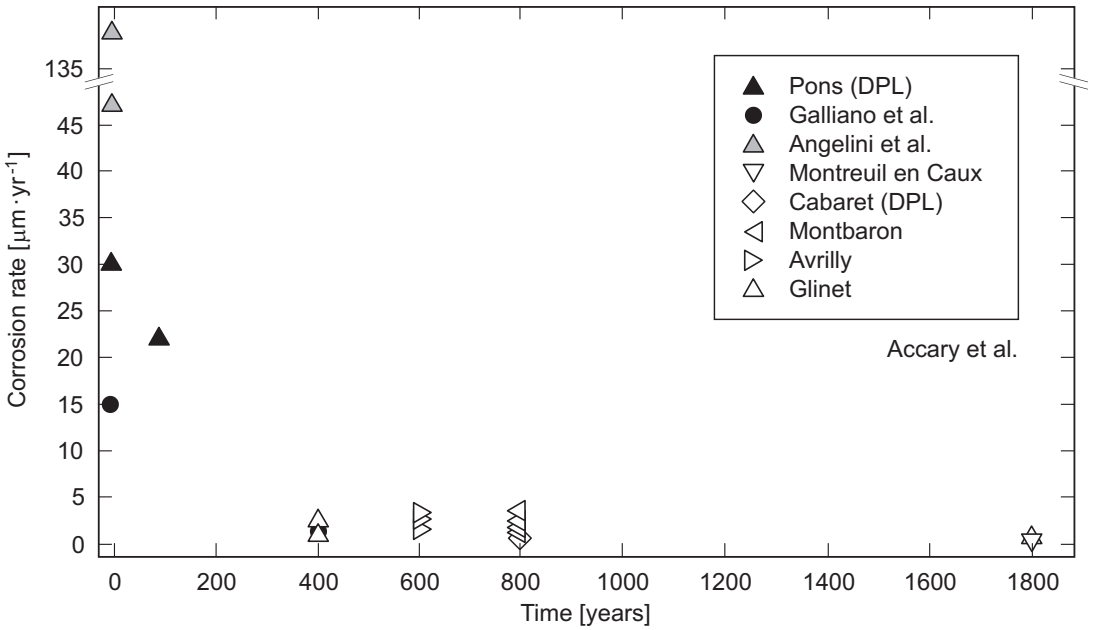

Figure 9: Comparison of inferred corrosion rates from artifacts examined by the authors (open symbols) and from literature data (full symbols) (Neff et al. 2006)

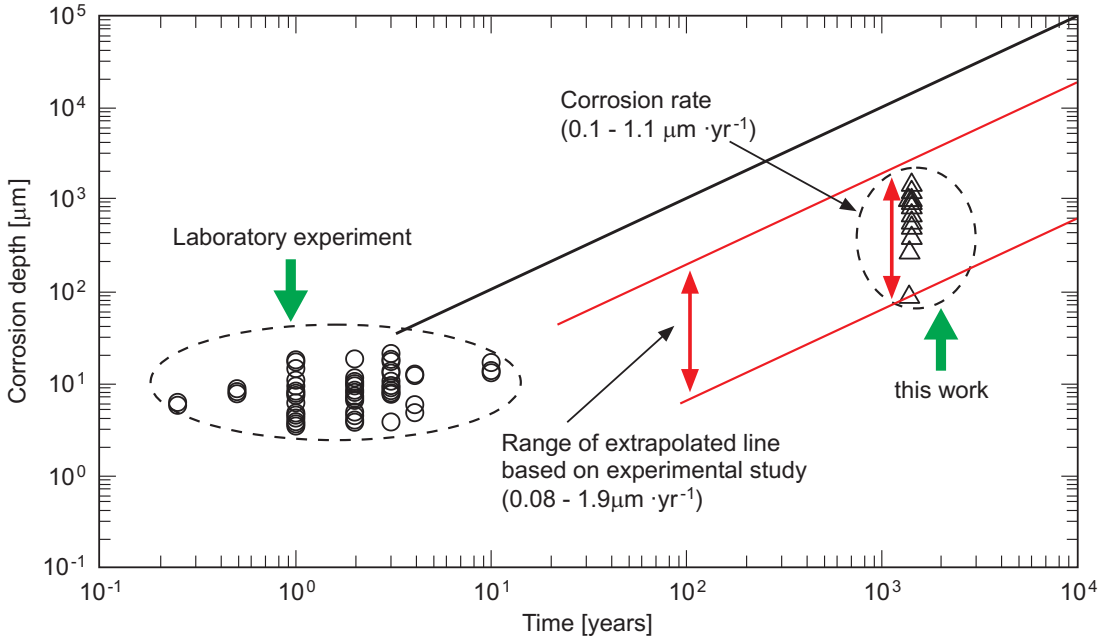

Figure 10: Comparison of extrapolated experimental corrosion rates and rates determined from artifacts from the Yamato Ancient Tomb (Yoshikawa et al. 2007)

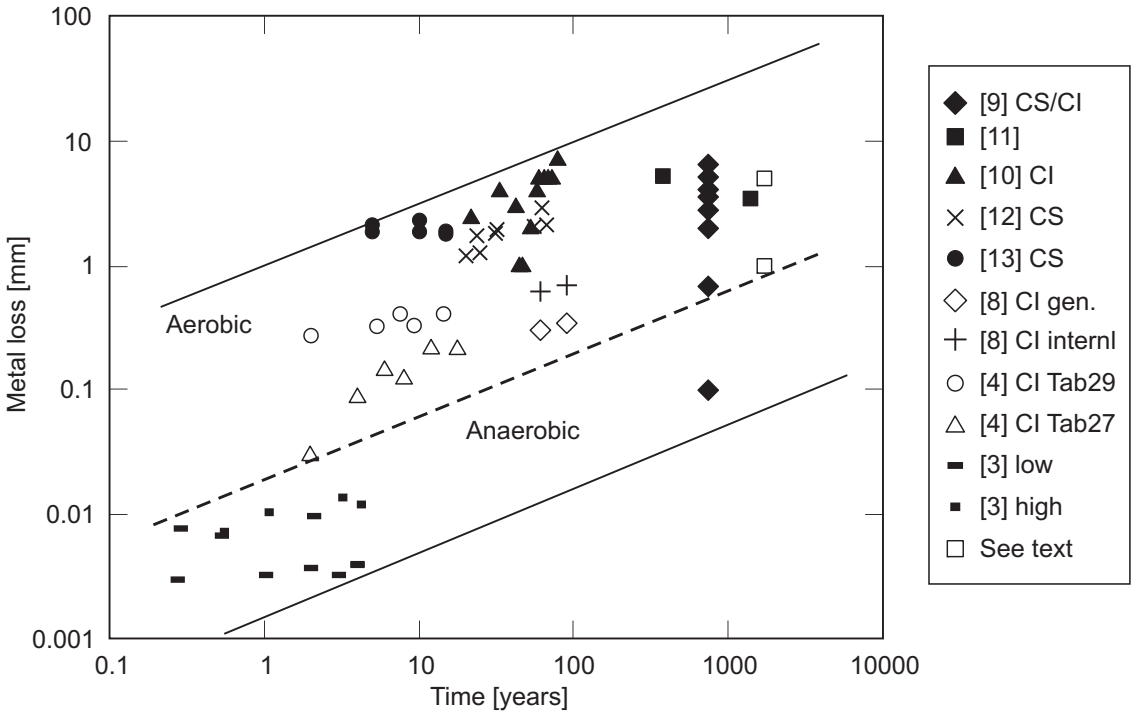

(a) in soil

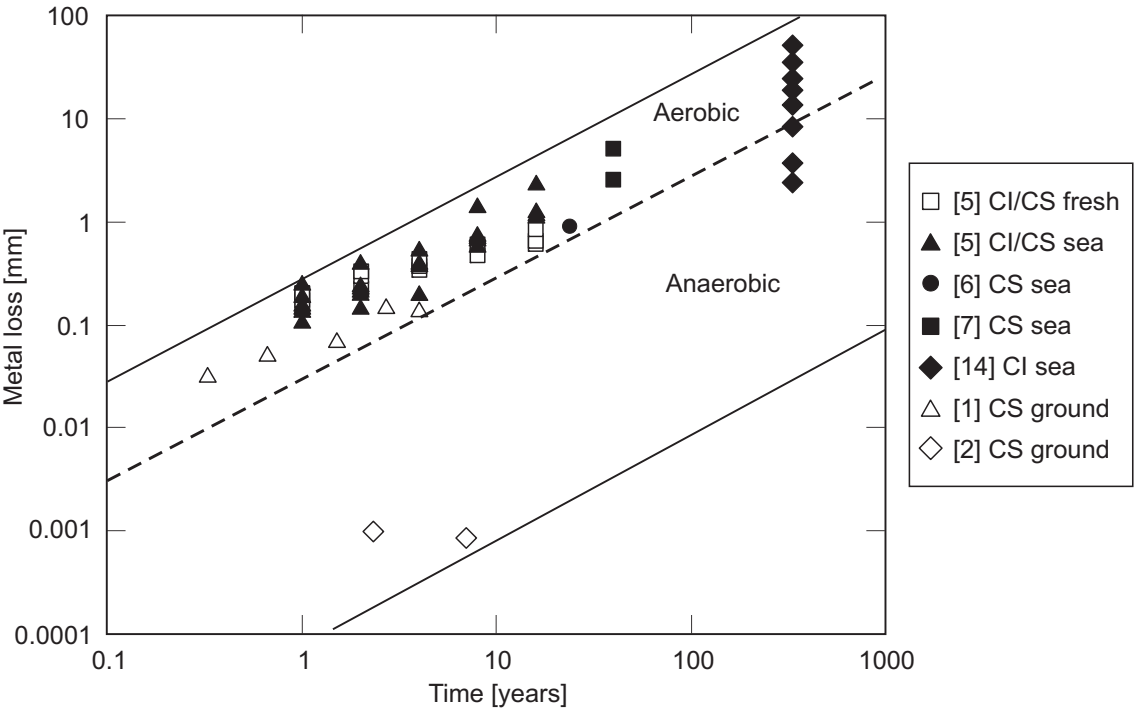

(b) in bulk solution

Figure 11: Compilation of corrosion rates of iron and steel exposed to soils and natural waters (Crossland 2005)

3 Mechanism of the anaerobic corrosion of C-steel

3.1 Electrochemical reactions

Under anaerobic conditions, the electrochemical reactions of interest are the anodic dissolution of Fe

$$Fe \rightarrow Fe^{2+} + 2e^- \quad (2)$$

and the cathodic reduction of H_2O

$$H_2O + e^- \rightarrow ½\ H_2 + OH^- \quad (3)$$

The overall corrosion reaction can be written as

$$Fe + 2H_2O \rightarrow Fe(OH)_2 + H_2 \quad (4)$$

As discussed in more detail below, species other than $Fe(OH)_2$ may precipitate depending upon the solution composition. Under some conditions, $Fe(OH)_2$ is transformed to Fe_3O_4 via the Schikkor reaction

$$3Fe(OH)_2 \rightarrow Fe_3O_4 + 2H_2O + H_2 \quad (5)$$

Alternatively, the formation of Fe_3O_4 can be written as

$$3Fe + 4H_2O \rightarrow Fe_3O_4 + 4H_2 \quad (6)$$

Magnetite formation is generally considered to be favoured at higher temperatures. It is interesting to note that all authors cite the early work of Linnenbom (1958) when referring to the temperature dependence of the Schikkor reaction. From this, it is apparent that little work has been done on the relative stability of $Fe(OH)_2$ and Fe_3O_4 since that time. However, based on references to this earlier work, it appears that the transformation of $Fe(OH)_2$ to Fe_3O_4 is favoured at temperatures above ~ 60 °C.

Reactions (3) to (6) have been written as irreversible because, although in principle the reverse reaction might occur at high H_2 partial pressure, no dependence of the corrosion rate or cathodic reaction on p_{H2} has been reported (Smart et al. 2001, 2002a). Neither the cathodic Tafel slope nor the corrosion current density (determined by Tafel extrapolation) varied systematically with the H_2 pressure (although some variability was observed) for pressures between 0.1 MPa and 9 MPa at temperatures of 24 °C and 80 °C. In addition, E_{CORR} was insensitive to p_{H2} under the same conditions indicating that the overall corrosion reaction is not cathodically limited by the rate of H_2 evolution. As noted in Section 2.1.1, the mass-loss corrosion rate did not vary systematically with p_{H2} either at pressures up to 10 MPa at 90 °C. (For reference, the equilibrium partial pressure for Reactions (4) and (6) are reported to be 10 – 14 MPa and 50 – 80 MPa, respectively, at room temperature, the variation due to uncertainty in the thermodynamic data (Platts et al. 1994, Simpson 1989).

3.2 Film structure and composition

In considering the available information on the film structure and composition during the long-term anaerobic corrosion of a C-steel canister it is important to take into account the evolution of environmental conditions within the repository. Prior to the establishment of cool anaerobic conditions, the canister will have been exposed to a period of aerobic redox conditions and elevated temperature. Therefore, the nature of the film during the long-term anaerobic period will inevitably be affected by this preceding period of transitory conditions.

3.2.1 Aerobic conditions

The nature of the film that forms under aerobic conditions is relevant here only inasmuch as the anaerobic phase in the repository is preceded by a period of aerobic corrosion. There are a large number of studies of the composition and structure of films formed on iron and steel under aerobic conditions. King and Stroes-Gascoyne (2000) reviewed the formation and transformation of Fe(II) and Fe(III) corrosion products on steel under conditions likely to exist in a deep geologic repository.

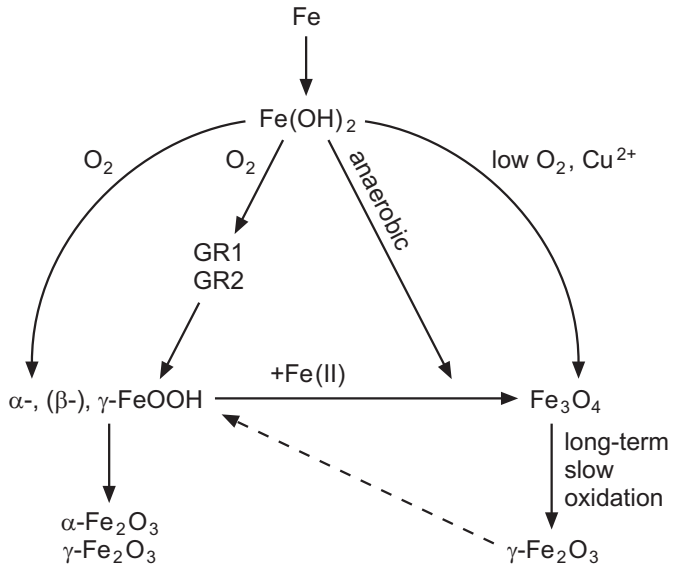

Figure 12: Generalized reaction scheme for the formation and transformation of corrosion product films on C-steel (King and Stroes-Gascoyne 2000)

Figure 12 shows a general scheme for the formation of various green rusts (GR), ferric oxyhydroxides, and oxides that could form, with the preferred products and reaction paths dependent on the environmental conditions (King and Stroes-Gascoyne 2000). Initial oxidation of Fe in neutral and slightly alkaline solutions generally leads to the formation of $Fe(OH)_2$. Under aerobic conditions, $Fe(OH)_2$ will be oxidized to produce an Fe(III)-containing corrosion product. Various authors have studied the oxidation of $Fe(OH)_2$ to α-, β- and γ-FeOOH and Fe_3O_4. Rapid oxidation in aerated solutions tends to produce one or more of the ferric hydroxides (Domingo et al. 1994), whereas slower oxidation in deaerated solutions produces Fe_3O_4 (Domingo et al. 1994, Odziemkowski et al. 1998). Slower oxidation is believed to allow time for incorporation of Fe^{2+} into the lattice, a process that is also supported by a slight excess of Fe(II) in solution. The stability of Fe_3O_4 is also increased at higher temperatures (Domingo et al. 1994). Conversely, the opposite factors favour the formation of either α-FeOOH (goethite) or γ-FeOOH (lepidocrocite) (the formation of β-FeOOH (akaganeite) is rarely reported).

In the presence of groundwater anions, oxidation of $Fe(OH)_2$ to FeOOH and Fe_3O_4 proceeds via intermediate compounds Green Rusts (Figure 12). Green Rust 1 (GR1) is formed in solutions containing planar ligands, such as Cl^-, Br^- and CO_3^{2-} (Refait and Génin 1993) and Green Rust 2 (GR2) is formed in solutions containing SO_4^{2-}. Green rusts are hydrated intermediate species containing various proportions of Fe(II), Fe(III) and the corresponding anion. The composition of GR1 formed in Cl^- solutions is reported to be $3Fe(OH)_2 \cdot Fe(OH)_2Cl \cdot nH_2O$ (Refait and Génin 1993), consisting of two ferrous species for each ferric ion. In SO_4^{2-} solutions, GR2 has a composition of $4Fe(OH)_2 \cdot 2FeOOH \cdot FeSO_4 \cdot nH_2O$, with a Fe(II) : Fe(III) ratio of 5 : 2 (Olowe and Génin 1989). The proportion of FeOOH and Fe_3O_4 in the final oxidation product is a sensitive function of the pH and concentration of anion.

3.2.2 Film transformation during the aerobic-anaerobic transitions

At the end of the aerobic phase, therefore, the canister surface will be covered by an Fe(III)-rich corrosion product layer that may contain various amounts of α- and γ-FeOOH, Fe_3O_4, and GR1 and GR2. Corrosion product films formed in natural systems tend to be spatially inhomogeneous, with these species distributed over the surface rather than being present as uniform layers.

As redox conditions within the repository become anaerobic, the Fe(III) phases within the corrosion product film will become thermodynamically unstable and will be reduced to predominantly Fe(II) species. The reduction of Fe(III) in corrosion products on C-steel surfaces has been studied in a number of systems, most notably in the reductive dissolution of Fe_3O_4 (e.g., Mancey et al. 1993). Corrosion products can be dissolved (transformed) both electrochemically (by reducing Fe(III) to Fe(II)) or chemically at acidic pH and in the presence of complexants for dissolved Fe. Of most interest here is the electrochemical reduction process, as the solubility of the Fe(III) solids in neutral to slightly alkaline bentonite pore-water solutions will be low.

Electrochemical reduction of Fe(III) species can proceed by one of two mechanisms, namely: (i) coupling of the oxidation of the underlying steel to reduction of the corrosion product or (ii) reaction between dissolved Fe(II) and the Fe(III) corrosion product. Figure 13 shows the expected evolution of the E_{CORR} of a C-steel canister as the environment in the repository evolves from aerobic to anaerobic. The transition period is characterized by a rapid decrease in E_{CORR}. Prior to this decrease the corrosion potential is determined by the redox potential between the Fe(III) corrosion products and dissolved Fe(II) and Fe(III) species in solution. As the underlying steel surface is exposed to the environment, oxidation of Fe couples with reduction of Fe(III)

$$Fe + 2\text{"Fe(III)"} \rightarrow 3\text{"Fe(II)"} \qquad (7)$$

where "Fe(III)" represents the Fe(III)-rich corrosion product formed during the aerobic phase and "Fe(II)" represents either dissolved ferrous ions or a secondary precipitated Fe(II) corrosion product. Eventually sufficient underlying steel is exposed that the potential is determined by the rates of Fe dissolution and H_2O reduction on the underlying surface and E_{CORR} attains a value representative of that in anaerobic solution. This type of transition has been observed not only for the reductive dissolution of Fe_3O_4 deposited in steam generators (Shoesmith et al. 1981) but also for the dissolution of millscale on pipeline steel (Qin et al. 2004).

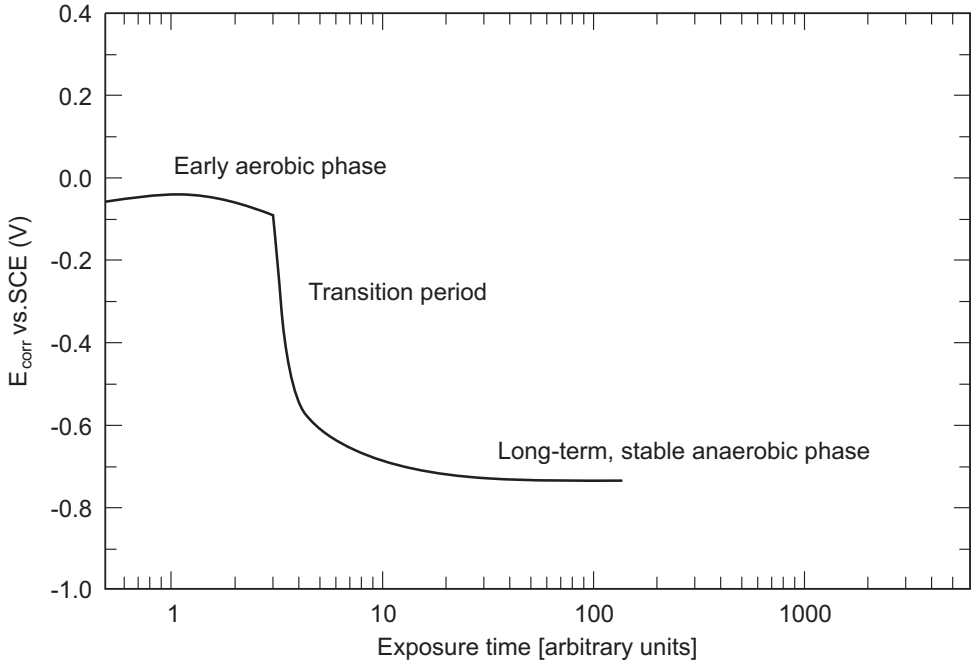

Figure 13: Schematic of expected evolution of the corrosion potential of a carbon steel canister

Various studies of the reduction of FeOOH by Fe(II) have been reported. Ishikawa et al. (1998) studied the reduction of α-, β- and γ-FeOOH by Fe(II) in Cl^- solutions as a function of temperature and $[OH^-]$:[Fe(II)] ratio. The reduction of γ-FeOOH by Fe(II) resulted in the complete conversion of the ferric species to Fe_3O_4 between 25 °C and 100 °C and pH 3 – 13. The reduction of βFeOOH resulted in the formation of Fe_3O_4 and α-FeOOH, whilst the reduction of α-FeOOH was sluggish with little apparent conversion to Fe_3O_4. Increasing temperature increased the amount of Fe_3O_4 formed. Overall, the relative ease of conversion was β-FeOOH > γ-FeOOH > α-FeOOH. Reduction of the ferric phase was believed to proceed via dissolved Fe(II) and Fe(III) species, the relative ease of conversion being directly related to the solubility of the various FeOOH polymorphs. Tamaura et al. (1983) also studied the reaction between Fe(II) and γ-FeOOH

$$Fe^{2+} + 2\gamma\text{-FeOOH} \rightarrow Fe_3O_4 + 2H^+ \quad (8)$$

The reaction was believed to proceed via two distinct steps, each involving a de-protonation process. Stratmann and Hoffman (1989) studied the reduction of α- and γ-FeOOH as a function of potential at 25 °C using *in situ* Mössbauer spectroscopy. At potentials between –0.2 and -0.4 V_{SHE}, γ-FeOOH is partially transformed to Fe_3O_4, although conversion appears complete towards the negative end of this potential range. At more negative potentials α-FeOOH is reduced.

3.2.3 Anaerobic conditions

As apparent from the discussion in Section 2.1, there are few detailed mechanistic studies of film formation during the anaerobic corrosion of C-steel in the nuclear waste management literature. Much of the information presented here, therefore, has been taken from electrochemical

studies of the passivation of Fe (or C-steel) in neutral or slightly alkaline solutions. In using this information, it is necessary to distinguish those processes that might occur at the open-circuit potential in anaerobic solution and those that occur under anodic polarization conditions. Furthermore, as noted above, in judging the relevance of this information we must further remember that the canister surface will have been pre-corroded during the aerobic transient before being exposed to anaerobic conditions.

A common medium for studying the passivity of C-steel electrochemically in mildly alkaline solution is the borate buffer system. An active/passive peak is observed during anodic polarization corresponding to the formation of a passive $Fe(OH)_2$ layer (Li et al. 2003, Ohtsuka and Yamada 1998, Tsuru et al. 1990, Vela et al. 1986). The peak potential shifts to more negative potentials by 60 mV/pH unit and has a potential of –0.66 V_{SCE} at pH 8.4 (Li et al. 2003, Vela et al. 1986). Díez-Pérez et al. (2001) propose that $Fe(OH)_2$ is responsible for passivation at these relatively negative potentials. At more positive potentials (and, quite possibly, more positive than those that will be attained during the anaerobic phase in the repository) different authors ascribe the observed passivity to a spinel phase related to Fe_3O_4 and γ-Fe_2O_3 with different octahedral, tetrahedral, and interstitial site occupancies (Davenport et al. 2000), γ-Fe_2O_3 (Ahn and Kwon 2004, Kim et al. 2001, Li et al. 2003), or a duplex inner Fe_3O_4 layer and outer hydrous Fe oxyhydroxide layer (Vela et al. 1986).

Odziemkowski et al. (1998) studied the anaerobic oxidation of iron particles in simulated dilute groundwater solutions at ambient temperature using normal and enhanced Raman spectroscopy. Magnetite was formed from a precursor $Fe(OH)_2$ phase, with conversion proceeding within a matter of a few ten's of hours even at room temperature. Growth of the Fe_3O_4 phase was believed to result from a dissolution-precipitation process, rather than by a high-field solid-state mechanism. To explain the increase in E_{CORR} observed during the experiment, Odziemkowski et al. (1998) propose that the anodic and cathodic reactions are spatially separated, with anodic dissolution occurring at the base of pores in the porous Fe_3O_4 layer and H_2O reduction occurring at the film/water interface.

The presence of Cl^- interferes with the formation of $Fe(OH)_2$ through a competition between OH^- and Cl^- ions in the initial oxidation of Fe (Ashley and Burstein 1991, MacFarlane and Smedley 1986). Thus, a mixed Cl^-/OH^- layer forms (Ashley and Burstein 1991), which would be expected to interfere with the formation of a passive $Fe(OH)_2$ layer or its transformation to Fe_3O_4. However, it is difficult to draw conclusions regarding the long-term effect of Cl^- on the passivity of C-steel based on its impact on the composition of the first oxidized monolayer.

Carbonate species will also be present in the bentonite pore water because of the dissolution of calcite impurities in the clay. Iron carbonate is only reported to be formed in a range of pH and potential values. In moderately alkaline carbonate solutions (> pH 9.5), $Fe(OH)_2$, Fe_3O_4 and γ-Fe_2O_3 species are reported by surface-enhanced Raman spectroscopy (Gui and Devine 1995, Simpson and Melendres 1996). Simpson and Melendres (1996) report the formation of $FeCO_3$ only at lower pH, at temperatures < 50 ^oC, and at potentials between –0.7 V_{SCE} and –0.5 V_{SCE}. Lee et al. (2006 a, b) report the formation of a porous $FeCO_3$ layer in carbonate-rich solutions. Open pores within the film were maintained by the complexation of Fe^{2+} by HCO_3^-, which prevented precipitation within the film. The formation of $FeCO_3$ films is of particular interest given the observation of this phase during corrosion experiments under simulated repository conditions in the presence of compacted bentonite (Papillon et al. 2003, Taniguchi et al. 2004).

Porous corrosion deposits are also associated with the formation of protective films on C-steel exposed to high-temperature water (Castle and Masterson 1966, Friggens and Holmes 1968, Park and Macdonald 1983). A duplex Fe_3O_4 layer is formed in this system, with a thin inner

layer formed by a solid-state process and a porous outer layer formed by a dissolution/precipitation mechanism. Porosity in the outer layer is maintained by the hydrolysis of cations and the consequent decrease in pH which prevents precipitation within the pores.

3.3 Film properties

3.3.1 Effect of corrosion products

There has been some debate about the effect of the accumulation of corrosion products on the long-term corrosion rate of C-steel canisters (Kojima et al. 1995, Taniguchi 2003). Kojima et al. (1995) simulated the long-term corrosion behaviour of C-steel by contacting C-steel coupons by compacted Fe_3O_4 powder (maintained in place by compacted bentonite) or by a compacted Fe_3O_4/bentonite mixture. In the case of a layer of compacted Fe_3O_4, the layer thickness was varied from 0 to 10 mm. For the Fe_3O_4/bentonite mixture, the magnetite content was varied from 0 to 50 wt.%. The compacted mixtures were saturated with a 3 wt.% NaCl solution. Two C-steel electrodes were used and the coupling current between the electrodes and the coupled potential were recorded. The polarization resistance R_P was measured at the end of the tests by EIS.

The presence of the Fe_3O_4 simulated corrosion product resulted in an increase in the corrosion rate and, in the case of the Fe_3O_4/bentonite mixture, the degree of localization of the attack. The corrosion rate increased with either increasing Fe_3O_4 content of the mixture or with the thickness of the Fe_3O_4 layer. In the latter case, the presence of the Fe_3O_4 layer ennobled the corrosion potential. Clearly, if this system reflects the reality of a corroding C-steel canister, the implication is that the corrosion rate could increase with time as corrosion product accumulates.

The reasons for the apparent increase in corrosion rate with Fe_3O_4 loading were not discussed by Kojima et al. (1995). However, it is possible that either (i) the reductive dissolution of the Fe_3O_4 powder was coupled to the oxidation of the C-steel coupon, or (ii) the simulated Fe_3O_4 corrosion product is acting as a large surface area cathode. The first explanation implies that a Fe_3O_4-covered C-steel system is metastable under these conditions and would revert, possibly, to a $Fe(OH)_2$ surface film. If correct then this effect would be transient and would not result in a permanently elevated corrosion rate. If, on the other hand, the Fe_3O_4 is acting as an external cathode coupled to the C-steel surface then the increased rate might not only be sustained but would tend to increase as corrosion proceeds and Fe_3O_4 continues to accumulate (provided the Fe_3O_4 retains electrical connectivity to the steel surface).

Taniguchi (2003) attempted to replicate the findings of Kojima et al. (1995) by immersing Fe wires in powdered magnetite in ampoules under strictly anaerobic conditions and measuring both the amount of H_2 produced and the change in Fe(III) : Fe(II) ratio in the corrosion product. Experiments were conducted in distilled water, 0.5 mol·dm^{-3} NaCl, and 0.1 mol·dm^{-3} $NaHCO_3$ solutions at 80 ^{o}C for periods of 30 – 90 days. The mass-loss corrosion rate was observed to increase with the loading of Fe_3O_4 powder, although not linearly (Figure 14). Also shown in Figure 14 is the equivalent corrosion rate based on the amount of H_2 found in the ampoule at the end of the test. The reduction of H_2O accounted for only about 30 % of the total mass loss, with the remainder resulting from the reduction of Fe(III) to Fe(II) in the magnetite powder, as determined after the test by titration. However, it is also apparent from Figure 14 that the presence of Fe_3O_4 did increase the amount of H_2 produced over that in the absence of the simulated corrosion product. Thus, it was concluded that much of the increase in corrosion rate reported by Kojima et al. (1995) was caused by the reduction of the Fe_3O_4 itself. Taniguchi (2003) also estimated the additional corrosion that might occur based on his measurements and concluded that the consequences would have a minimal impact on the canister lifetime.

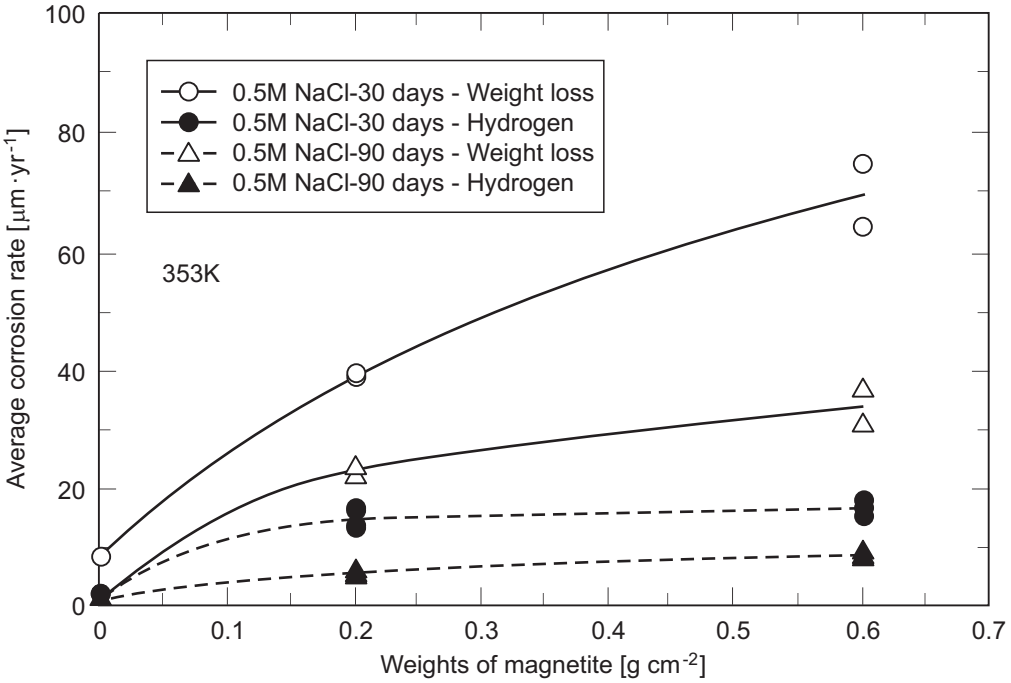

Figure 14: Dependence of the mass-loss corrosion rate on the magnetite loading in 0.5 mol dm^{-3} NaCl solution (Taniguchi 2003)

Fushimi et al. (2002) used scanning electrochemical microscopy to study the generation of H_2 from a galvanic couple between C-steel and a Fe_3O_4 single crystal in pH 5.8 sulphate solution. The SECM was used to determine the amount of H_2 generated in solution above the Fe_3O_4 crystal, from which it was concluded that H_2O reduction on Fe_3O_4 accounted for ~ 50 % of the coupled current measured between the two electrodes. These measurements confirm, therefore, that H_2O is reduced on Fe_3O_4.

The enhancement of the H_2 evolution reaction on Fe(III)/Fe(II) corrosion products has also been reported by Been et al. (2007). Figure 15 shows steady-state current-potential behaviour for three different steel surface conditions, namely: a polished and cathodically pre-cleaned surface, a polished surface pre-oxidized for 5 minutes at –0.7 V_{SCE}, and millscale-covered surfaces comprising a mixture of $FeCO_3$ and Fe_3O_4. Experiments were performed in a dilute simulated groundwater purged with 5 vol.% CO_2/N_2 (~ pH 6.5). The rate of H_2O reduction is enhanced at moderately cathodic potentials (up to approximately –0.95 V_{SCE}) on both the millscale and pre-oxidized surfaces, but this catalytic activity is lost on the pre-oxidized surface at more-negative potentials. Enhanced H_2 evolution is maintained on the millscale-covered electrodes. This enhanced H_2 evolution is believed to be catalyzed by Fe(III)/Fe(II) active sites on the surface which, on the pre-oxidized surface, are lost if the electrode is polarized too negatively. Large cathodic Tafel slopes (~ 200 mV) are observed which reflect not only the kinetics of H_2O reduction but also the potential dependence of the number of active Fe(III)/Fe(II) surface sites.

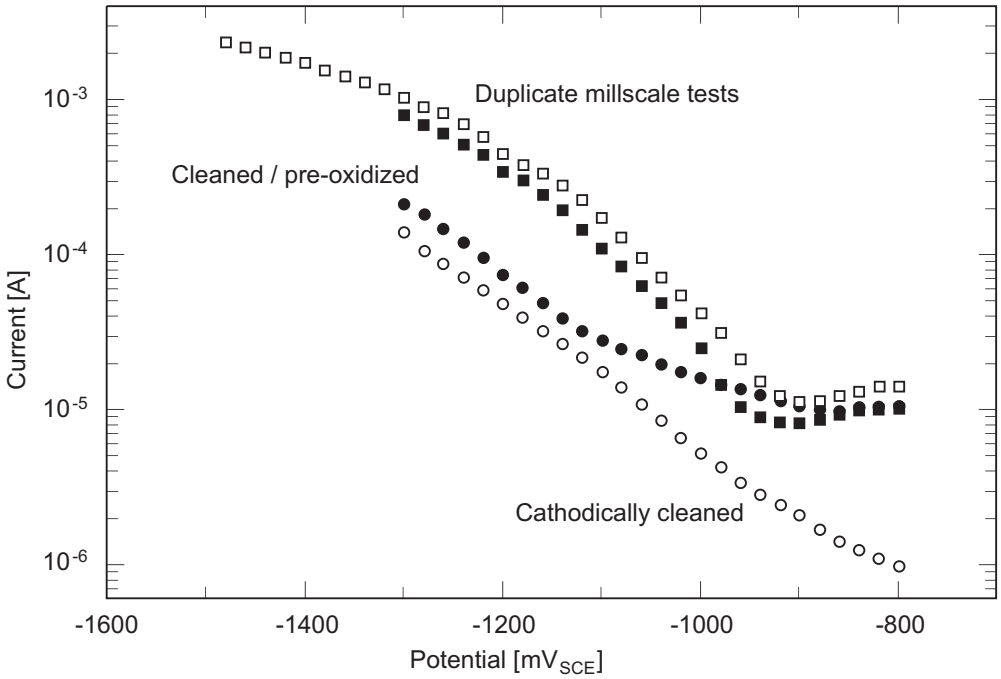

Figure 15: Steady-state cathodic polarization curves for hydrogen evolution on various steel surfaces in dilute synthetic groundwater at ~ pH 6.5 (Been et al. 2007)

However, even if such a mechanism is relevant to the compact Fe_3O_4 layers that might form on a canister surface, the process is inherently self-stifling. As corrosion proceeds the Fe_3O_4 will be progressively reduced to an Fe(II)-dominant secondary phase which would ultimately shut down the process. Since Fe(III) reduction accounts for ~ 50 – 70 % of the additional corrosion observed then the period of enhanced corrosion should be transitory.

3.3.2 Mechanical and physical properties

The expansion of corrosion products is an important process both from the viewpoint of the generation of stresses in the canister shell and the possibility of spalling of the protective oxide.

Considerable effort has been expended in the Swedish program to determine the stresses that might arise between the outer Cu shell and inner cast iron insert of a failed canister due to expansion of the iron corrosion products (Smart et al. 2006a). Stacks of alternating copper and C-steel or cast iron discs were confined under a compressive load representative of that expected in a repository and immersed in deaerated simulated groundwater at 69 ^{o}C. The expansion of the stack was measured using displacement transducers. In separate experiments, C-steel and cast iron coupons were corroded under anaerobic conditions at 50 ^{o}C and 80 ^{o}C and the mechanical properties and structure of the oxide measured using AFM. Chemical composition of the film was determined by Raman and XPS.

No expansion of the test cells was observed over periods of up to 380 days. Expansion of the stack of coupons was observed if a low compressive load, smaller than that expected in a repository, was applied under cyclic wet-dry conditions. This latter test confirmed that the experimental technique worked and that expansion of unconfined (or weakly confined) coupons does occur. Surface analysis of the samples indicated the presence of Fe_3O_4, although α-FeOOH (goethite) and Fe_2O_3 were also detected by XPS, possibly because of air exposure during transfer of the samples to the instrument.

The absence of any observed expansion under realistic confining loads may be explained by the mechanical properties of the oxide. The AFM data suggest that the oxide is compliant and has a low Young's modulus in the range 0.04 – 2 MPa, approximately 2 – 4 orders of magnitude lower than that for Fe_3O_4 formed at high temperatures (Smart et al. 2006a), possibly as a result of the higher water content of the oxide formed at lower temperature.

In support of the absence of expansion effects observed experimentally, Smart and Adams (2006) examined a number of archaeological and industrial artifacts in which copper alloys in contact with steel or iron have been exposed to corrosive environments. In none of these cases was there any evidence for deformation caused by expansion of corrosion products.

Even if the growth and expansion of corrosion products is insufficient to induce strain in the canister shell, it is possible that such expansion will cause protective corrosion products to spall from the surface. This, in turn, might result in an increase in corrosion rate. No detailed studies of the spalling of oxides under anaerobic conditions or the effect on the corrosion rate were found in the literature under repository-relevant conditions.

However, there are a number of indirect observations that suggest that, even if spalling should occur, the corrosion rate will not increase significantly. First, there were no indications of an increase in H_2 generation rate due to spalling of corrosion products during the experiments of Schenk (1988), Simpson et al. (1985), or Smart et al. (2001, 2002b). Schenk (1988) did observe spikes in the H_2 generation rate, but these were ascribed to localized corrosion in some solutions rather than the sudden loss of protectiveness of the oxide film. Furthermore, in one test Smart et al. (2001) mechanically removed the outer layer of oxide by rubbing the coupon with a paper tissue. When the sample was returned to the test solution, there was only a temporary modest increase in the H_2 generation rate, suggesting that removal of the outer part of the protective film did not affect the protectiveness of the inner layer of what was presumed to be a duplex Fe_3O_4 film. In addition, scratching electrode tests showed rapid re-passivation (Smart et al. 2001), again suggesting a rapid film repair mechanism.

3.4 Rate-controlling process

The nature of the rate-controlling process for the anaerobic corrosion of C-steel can be inferred from the results of a number of the studies reported above.

The anaerobic corrosion rate of C-steel decreases with time due to the formation of a protective corrosion product layer. The exact nature and identity of this film is uncertain, but the most likely composition is either Fe_3O_4 (Smart et al. 2001) or, in the presence of high [HCO_3^-/CO_3^{2-}] and/or compacted bentonite, $FeCO_3$ (Lee et al. 2006a, b; Papillon et al. 2003; Taniguchi et al. 2004). A duplex structure has been inferred for the film (possibly comprising an inner layer overlaid by a porous $Fe(OH)_2$, $FeCO_3$, or (with increasing temperature) Fe_3O_4 layer, but no direct surface analytical evidence has been provided for this duplex structure (Smart et al. 2001).

The observation that the corrosion rate decreases as the corrosion potential shifts to more-positive values (Smart et al. 2001, 2002a) is consistent with a combination of kinetically controlled H_2 evolution and anodic dissolution under passive conditions, in which the anodic reaction is rate controlling. The rate-determining step, therefore, is likely the transport of a species across the surface film, but whether it is the diffusion of anions to the metal/film interface or the diffusion of cations in the other direction is unknown. Smart et al. (2001; 2002a, b) concluded that the corrosion rate is anodically controlled by ion transport across the inner barrier layer of a duplex Fe_3O_4 film on the surface.

Further evidence of anodic control is the absence of any effect on E_{CORR} or the corrosion rate of elevated H_2 partial pressures (Smart et al. 2001, 2002a). In addition, Simpson (1989) found that adsorption of Fe(II) by bentonite paste leads to an increase in corrosion rate by interfering with the formation of a precipitated protective layer. Although the presence of compacted bentonite will also lead to Fe(II) adsorption, the effect that this has on the rate of precipitation may be offset by the restrictive mass-transport conditions.

For Fe_3O_4-covered surfaces, there is some evidence that the cathodic reduction of H_2O occurs at the film/solution interface (Fushimi et al. 2002, Been et al. 2007). Hydrogen evolution may also occur on the C-steel surface (or at least the surface of the inner layer of a duplex film) at defects in the (outer) film. A similar effect would not be expected for non-conducting $FeCO_3$ films.

4 Summary

The current review has helped reduce the apparent variability in reported anaerobic corrosion rates. A number of the mass-loss corrosion rates compiled by Johnson and King (2003) may include effects due to entrained O_2, particularly those measured using the refreshed system of Simpson and co-workers and those for the initially aerated system of Lanza and Ronsecco (1986). In addition, the reported "steady-state" rates reported by Simpson et al. (1985) on the basis of short-term H_2-generation data are conservatively high, since later work by Kreis and Simpson (1992) clearly showed that it takes > 4,000 hr to achieve steady-state conditions.

There is a significant body of evidence from apparently well-conducted experiments that indicate an anaerobic corrosion rate of the order of $1 – 2$ μm·yr^{-1} in systems containing compacted clay. In bulk solution, long-term corrosion rates of the order of 0.1 μm·yr^{-1} have been reported. These experiments include measurements in both simulated and natural groundwaters (Kreis and Simpson 1992, Smart et al. 2001) and in compacted bentonite systems (Taniguchi et al. 2004). There are, however, a number of measurements indicating higher corrosion rates (in the range $1 – 5$ μm·yr^{-1}) (Marsh and Taylor 1988, Papillon et al. 2003). The continued decrease in corrosion rate over periods of up to 4 years (Taniguchi et al. 2004) suggests that any such tests should be carried out over periods of years rather than months in order to provide reliable long-term rates. In this regard, useful supporting information can be obtained from the study of archaeological artifacts.

The decrease in corrosion rate with time is due to the formation of a protective corrosion product film. The rate of corrosion appears to be anodically limited by transport of species across this film. Cathodic reduction of H_2O is not rate controlling, and may occur at the film/solution interface on Fe_3O_4-covered surfaces.

The formation of a duplex film has been proposed, with an inner layer overlaid by a $Fe(OH)_2$, $FeCO_3$, or Fe_3O_4 outer layer. Magnetite films appear to be favoured in bulk solution, especially at higher temperatures, whereas $FeCO_3$ is found in either high [HCO_3^-/CO_3^{2-}] solutions or in the presence of compacted bentonite.

There are a number of differences between the corrosion behaviour in bulk solution and in compacted clay. In bulk solution, the corrosion rate reaches an apparent steady state after ~ 6 months (Kreis and Simpson 1992), whereas no such condition is achieved after as long as 4 years in compacted clay (Taniguchi et al. 2004). The respective corrosion rates after these periods are ~ 0.1 μm·yr^{-1} in bulk solution and ~ $1 – 2$ μm·yr^{-1} in compacted clay. Corrosion films tend to be thinner and more compact on surfaces exposed to bulk solution.

In relating the results of laboratory studies under anaerobic conditions to the development of films on the canister surface, it is important to remember that the canister will have previously been exposed to a period of aerobic corrosion. Growth of the film under anaerobic conditions will initially occur through transformation of this pre-existing Fe(III)-rich film. Subsequent film growth under anaerobic conditions may be affected by this prior film transformation.

Film transformation is most likely to involve the reductive dissolution of Fe(III) films, either by galvanic coupling of C-steel dissolution and film reduction or by reaction between dissolved Fe(II) and the Fe(III)-rich film.

There is some evidence that the presence of Fe_3O_4 corrosion products could increase the rate of C-steel corrosion during the transition from aerobic to anaerobic conditions. The observed

corrosion rate enhancement is primarily due to the reduction of Fe(III) in the simulated Fe_3O_4 corrosion product, although enhanced H_2 evolution on the Fe_3O_4 is also observed. This enhancement mechanism cannot be sustained in the long term.

There is no evidence that periodic spalling of corrosion products will lead to an increase in corrosion rate. No such events have been observed in laboratory studies over periods of up to 4 years (based on immersion-type tests) and what evidence there is suggests that the inner layer of the postulated duplex structure may be the primary corrosion barrier. This inner layer is less likely to spall than a growing outer layer. Furthermore, hydrated corrosion products grown under anaerobic conditions are compliant and exhibit low Young's modulus. Therefore, it is not expected that high stresses could develop in such films. Futhermore, corrosion rates of archaeological artifacts are of the same order as the rates of steel corrosion in bentonite quoted above, which would not be the case if spalling of corrosion films plays an important role in determining the long-term corrosion rate.

Acknowledgements

The author wishes to acknowledge the helpful review comments of N. Smart (Serco Technical Assurance Services) and B. Kursten (SCK·CEN). The report also benefited from useful discussions with the members of Nagra's Canister Materials Review Board (D. Landolt (Swiss Federal Institute of Technology), D. Shoesmith (University of Western Ontario), J. Payer (Case Western Reserve University) and A. Davenport (University of Birmingham)). The assistance of L. Johnson for handling the review and editorial aspects is appreciated.

References

Ahn, S.J. and H.S. Kwon. 2004. Effects of solution temperature on electronic properties of passive film formed on Fe in pH 8.5 borate buffer solution. Electrochim. Acta 49, 3347-3353.

Ashley, G.W. and G.T. Burstein. 1991. Initial stages of the anodic oxidation of iron in chloride solutions. Corrosion 47, 908-916.

Been, J., H. Lu, F. King, T. Jack and R. Sutherby. 2007. The role of hydrogen in EAC of pipeline steels in near-neutral pH environments. In Environment-Induced Cracking of Materials. Volume 2: Prediction, Industrial Developments and Evaluation, S.A. Shipilov, R.H. Jones, J.-M. Olive, and R.B. Rebak (eds.), Elsevier (Amsterdam), p. 255–266.

Bracke, G., Müller, and K. Kugel. 2004. Derivation of gas generation rates for the Morsleben radioactive waste repository (ERAM). Unknown source.

Carlson, L., O. Karnland, S. Olsson, A. Rance, and N. Smart. 2006. Experimental studies on the interactions between anaerobically corroding iron and bentonite. Posiva Working Report 2006-60.

Castle, J.E. and H.G. Masterson. 1966. The role of diffusion in the oxidation of mild steel in high temperature aqueous solutions. Corros. Sci. 6, 93-104.

Crossland, I. 2005. Long term corrosion of iron and copper. In ICEM'05: 10th International Conference on Environmental Remediation and Radioactive Waste Management, September 4–8, 2005 (American Society of Mechanical Engineers, New York, NY), paper ICEM05-1272.

Crossland, I. 2006. Corrosion of iron-based alloys – evidence from nature and archaeology. Crossland Report CCL/2006/02, Nirex Ltd, Harwell, UK.

Crusset, D., F. Plas, A. Desestret, G. Santarini, J.-M. Gras, D. Féron, P. Combrade, and G. Pinard-Legry. 2001. Materials Baseline – Volume 4: Corrosion of metallic materials, Report No. C.RP.AMAT. 01.060, ANDRA, Châtenay-Malabry, France.

Davenport, A.J., L.J. Oblonsky, M.P. Ryan, and M.F. Toney. 2000. The structure of the passive film that forms on iron in aqueous environments. J. Electrochem. Soc. 147, 2162-2173.

Debruyn, W., J. Dresselaers, Ph. Vermieren, J. Kelchtermans and H. Tas. 1991. Corrosion of container and infrastructure materials under clay repository conditions. Commission of the European Communities Report, EUR 13667 EN.

Díez-Pérez, I., P. Gorostiza, F. Sanz, and C. Müller. 2001. First stages of electrochemical growth of the passive film on iron. J. Electrochem. Soc. 148, B307-B313.

Domingo, C., R. Rodriguez-Clemente and M. Blesa. 1994. Morphological properties of α-FeOOH, γ-FeOOH and Fe_3O_4 obtained by oxidation of aqueous Fe(II) solutions. J. Coll. Interface Sci. 165, 244-252.

Dong, J., T. Nishimura, and T. Kodama. 2001. Proc. 48th Japan Conf. On Materials and Environments, p. 321.

Dridi, W. 2005. Couplage entre corrosion et comportement diphasique dans un milieu poreux: Application à l'évolution d'un stockage des déchets radioactifs. Thèse présentée pour l'obtention du diplôme de docteur de l'École Nationale des Ponts et Chaussées.

Friggens, H.A. and D.R. Holmes. 1968. Nucleation and growth of magnetite films on Fe in high-temperature water. Corros. Sci. 8, 871-881.

Fushimi, K., T. Yamamuro, and M. Seo. 2002. Hydrogen generation from a single crystal magnetite coupled galvanically with a carbon steel in sulfate solution. Corros. Sci. 44, 611-623.

Gould, A.J. and U.R. Evans. J. Iron and Steel Inst. 155, 195.

Gras, J.-M. 1996. Résistance à la corrosion des matériaux de conteneur envisagés pour le stockage profond des déchets nucléaires – 1ère partie: aciers non ou faiblement alliés, fontes. Report No. EDF HT-40/96/002/A, Electricité de France, Moret-sur-Loing, France.

Gui, J. and T.M. Devine. 1995. A SERS investigation of the passive films formed on iron in mildly alkaline solutions of carbonate/bicarbonate and nitrate. Corros. Sci. 37, 1177-1189.

Ishikawa, T., Y. Kondo, A. Yasukawa and K. Kandon. 1998. Formation of magnetite in the presence of ferric oxyhydroxides. Corrosion Science 40, 1239–1251.

Jelenik, J. and P. Neufeld. 1982. Corrosion 38, 98.

JNC. 2000. H12: Project to establish the scientific and technical basis for HLW disposal in Japan. Japan Nuclear Cycle Development Institute, Supporting Report 2, Repository Design and Engineering Technology.

Johnson, L.H. and F. King. 2003. Canister options for the disposal of spent fuel. Nagra Technical Report 02-11. Nagra, Wettingen, Switzerland.

Kim, J.S., E.A. Cho, and H.S. Kwon. 2001. Photoelectrochemical study on the passive film on Fe. Corros. Sci. 43, 1403-1415.

King, F. and S. Stroes-Gascoyne. 2000. An assessment of the long-term corrosion behaviour of C-steel and the impact on the redox conditions inside a nuclear fuel waste disposal container. Ontario Power Generation Nuclear Waste Management Division Report No: 06819-REP-01200-10028.

King, F., C.D. Litke and S.R. Ryan. 1992. A mechanistic study of the uniform corrosion of copper in compacted Na-montmorillonite/sand mixtures. Corrosion Science 33, 1979–1995.

Kojima, Y., T. Hioki, and S. Tsujikawa. 1995. Simulation of the state of carbon steel n years after disposal with n years of corrosion product on its surface in a bentonite environment. Mat. Res. Soc. Symp. Proc. 353, 711-718.

Kreis, P. and J.P. Simpson. 1992. Hydrogen gas generation from the corrosion of iron in cementitious environments. In Corrosion Problems Related to Nuclear Waste Disposal, European Federation of Corrosion Publication Number 7 (Institute of Materials, London), 57-72.

Kursten, B. and P. Van Iseghem. 1999. In situ corrosion studies on candidate container materials for the underground disposal of high-level radioactive waste in boom clay. In Corrosion/99, NACE International (Houston, TX), paper no. 473.

Kursten, B., B. Cornélis, S. Labat, and P. Van Iseghem. 1996. Geological disposal of conditioned high-level and long lived radioactive waste. In situ corrosion experiments. SCK-CEN Report R-3121.

Landolt, D., A. Davenport, J. Payer and D.W. Shoesmith. 2009. A Review of Materials and Corrosion Issues Regarding Canisters for Disposal of Spent Fuel and High-level Waste in Opalinus Clay, Nagra Technical Report NTB 09-02. Nagra, Wettingen, Switzerland.

Lanza, F. and C. Ronsecco. 1986. Corrosion of low-carbon steel in clay and sea sediments. Commission of the European Communities Report EUR 10522 EN.

Lee, C.T., Z. Qin, M. Odziemkowski, and D.W. Shoesmith. 2006a. The influence of groundwater anions on the impedance behaviour of carbon steel corroding under anoxic conditions. Electrochim. Acta 51, 1558–1568.

Lee, C.T., M.S. Odziemkowski, and D.W. Shoesmith. 2006b. An in situ Raman-electrochemical investigation of carbon steel corrosion in $Na_2CO_3/NaHCO_3$, Na_2SO_4, and NaCl solutions. J. Electrochem. Soc. 153, B33–B41.

Li, W.S., S.Q. Cai, and J.L. Luo. 2003. Electrochemical investigation on passivation process of iron in borate buffer solution. In Proc. Environmental Degradation of Materials & Corrosion Control in Metals (EDMCCM), J. Luo, M. Elboujdaini, D. Shoesmith, and P.C. Patnaik (eds.) (Canadian Institute if Mining, Metallurgy and Petroleum, Montreal, PQ), pp. 55-70.

Linnenbom, V.J. 1958. J. Electrochem. Soc. 105, 321.

MacFarlane, D.R. and S.I. Smedley. 1986. The dissolution mechanism of iron in chloride solutions. J. Electrochem. Soc. 133, 2240-2244.

Mancey, D.S., D.W. Shoesmith, J. Lipkowski, A.C. McBride and J. Noël. 1993. An electrochemical investigation of the dissolution of magnetite in acidic electrolytes. Journal of the Electrochemical Society 140, 637–642.

Marsh, G.P. and K.J. Taylor. 1988. An assessment of carbon steel containers for radioactive waste disposal. Corrosion Science 28, 289-320.

Marsh, G.P., I.W. Bland, J.A. Desport, C. Naish, C. Wescott, and K.J. Taylor. 1983. Corrosion assessment of metal overpacks for radioactive waste disposal. European Appl. Res. Rept.-Nucl. Sci. Technol. 5, 223-252.

Marsh, G.P., A.H. Harker, and K.J. Taylor. 1989. Corrosion of carbon steel nuclear waste containers in marine sediment. Corrosion 45, 579-589.

Nagra. 2002. Project Opalinus Clay. Safety Report. Nagra Technical Report NTB 02-05. Nagra, Wettingen, Switzerland.

Nagra (2008c): Bericht zum Umgang mit den Empfehlungen in den Gutachten und Stellungnahmen zum Entsorgungsnachweis, Nagra NTB 08-03 (in German). Nagra, Wettingen, Switzerland.

Neff, D., P. Dillmann, M. Descostes, and G. Beranger. 2006. Corrosion of iron archaeological artefacts in soil: Estimation of the average corrosion rates involving analytical techniques and thermodynamic calculations. Corros. Sci. 48, 2947-2970.

Odziemkowski, M.S., T.T. Schumacher, R.W. Gillham and E.J. Reardon. 1998. Mechanism of oxide film formation on iron in simulating groundwater solutions: Raman spectroscopic studies. Corrosion Science 2/3, 371–389.

Ohtsuka, T. and H. Yamada. 1998. Effect of ferrous ion in solution on the formation of anodic oxide film on iron. Corrosion Science 40, 1131-1138.

Olowe, A.A. and J.M.R. Génin. 1989. Influence of temperature and initial ratio of the reactants on the formation of rusts in sulphated media. Hyperfine Interactions 46, 445–452.

Papillon, F., M. Jullien, and C. Bataillon. 2003. Carbon steel behaviour in compacted clay: two long term tests for corrosion prediction. In Prediction of Long Term Corrosion Behaviour in Nuclear Waste Systems. European Federation of Corrosion Publication No. 36 (Institute of Materials, Minerals and Mining, London), p. 439–454.

Park, J.R. and D.D. Macdonald. 1983. Impedance studies of the growth of porous magnetite films on carbon steel in high temperature aqueous systems. Corrosion Science 23, 295–315.

Peat, R. S. Brabon, P.A.H. Fennell, A.P. Rance, and N.R. Smart. 2001. Investigation of Eh, pH and corrosion potential of steel in anoxic groundwater. SKB Technical Report TR-94-01.

Platts, N., D.J. Blackwood, and C.C. Naish. 1994. Anaerobic oxidation of carbon steel in granitic groundwaters: A review of the relevant literature. SKB Technical Report TR-01-01.

Qin, Z., B. Demko, J. Noël, D. Shoesmith, F. King, R. Worthingham and K. Keith. 2004. Localized dissolution of millscale-covered pipeline steel surfaces. Corrosion 60, 906-914.

Rance, A.P., R. Peat, and N.R. Smart. 2004. Analysis of electrochemistry cells. SKB Technical Report TR-04-01.

Refait, Ph. And J.-M.R. Génin. 1993. The oxidation of ferrous hydroxide in chloride-containing aqueous media and Pourbaix diagrams of Green Rust One. Corrosion Science 34, 797-819.

Schenk, R. 1988. Untersuchungen über die Wasserstoffbildung durch Eisenkorrosion unter Endlagerbedingungen. National Cooperative for the Storage of Radioactive Waste Technical Report, Nagra NTB 86-24.

Seo, M., G. Hultquist, L. Grasjo, and N. Sato. 1987. Proc. 10th Int. Conf. On Metallic Corrosion, paper 231, p. 481.

Shoesmith, D.W., W. Lee, and D.S. Owen. 1981. Power Industry Res. 1, 253.

Simpson, J.P. 1984. Experiments on container materials for Swiss high-level waste disposal projects, Part II. National Cooperative for the Storage of Radioactive Waste Technical Report, Nagra NTB 84-01. Nagra, Wettingen, Switzerland.

Simpson, J.P. 1989. Experiments on container materials for Swiss high-level waste disposal projects, Part IV. National Cooperative for the Storage of Radioactive Waste Technical Report, Nagra NTB 89-19. Nagra, Wettingen, Switzerland.

Simpson, J.P. and P.-H. Valloton. 1986. Experiments on container materials for Swiss high-level waste disposal projects, Part III. Nagra Technical Report NTB 86-25. Nagra, Wettingen, Switzerland.

Simpson, J. and J. Weber. 1992. Steel as a container material for nuclear waste disposal. In Corrosion Problems Related to Nuclear Waste Disposal, European Federation of Corrosion Publication Number 7 (Institute of Materials, London), 43-56.

Simpson, J.P., R. Schenk, and B. Knecht. 1985. Corrosion rate of unalloyed steels and cast irons in reducing granitic groundwaters and chloride solutions. Mat. Res. Soc. Symp. Proc. 50, 429-436.

Simpson, L.J. and C.A. Melendres. 1996. Surface-enhanced Raman spectroelectrochemical studies of corrosion films on iron in aqueous carbonate solution. J. Electrochem. Soc. 143, 2146-2152.

Smailos, E., W. Schwarzkopf, B. Fiehn and R. Köster. 1985. Corrosion behaviour of container materials in saliferous environments. Commission of European Communities Report, EUR-9570/1985.

Smart, N.R. and R. Adams. 2006. Natural analogues for expansion due to the anaerobic corrosion of ferrous materials. SKB Technical Report TR-06-44.

Smart, N.R., D.J. Blackwood, and L.O. Werme. 2001: The anaerobic corrosion of carbon steel and cast iron in artificial groundwaters. SKB Technical Report TR-01-22.

Smart, N.R., D.J. Blackwood, and L.O. Werme. 2002a. Anaerobic corrosion of carbon steel and cast iron in artificial groundwaters: Part 1 – electrochemical aspects. Corrosion 58, 547-559.

Smart, N.R., D.J. Blackwood, and L.O. Werme. 2002b. Anaerobic corrosion of carbon steel and cast iron in artificial groundwaters: Part 2 – gas generation. Corrosion 58, 627-637.

Smart, N.R., A.P. Rance, and L.O. Werme. 2004. Anaerobic corrosion of steel in bentonite. Mat. Res. Soc. Symp. Proc. 87, 441–446.

Smart, N.R., A.P. Rance, and P.A.H. Fennell. 2006a. Expansion due to the anaerobic corrosion of iron. SKB Technical Report TR-06-41.

Smart, N.R., A.P. Rance, L. Carlson, and L.O. Werme. 2006b. Further studies of the anaerobic corrosion of steel in bentonite. Mat. Res. Soc. Symp. Proc. 932, 813–820.

Smart, N.R., F. Bate, L. Carlson, M.R. Cave, K. Green, T.G. Heath, A.R. Hoch, F. M. I. Hunter, O. Karnland, S.J. Kemp, A.E. Milodowski, S. Olsson, A. M. Pritchard, A. P. Rance, R.A Shaw, H. Taylor, B Vickers, L. O. Werme, and C.L. Williams. 2008. Interactions Between Iron Corrosion Products And Bentonite, Serco/TAS/MCRL/19801/C001 Issue 2.

Stratmann, M. and K. Hoffmann. 1989. *In situ* Mößbauer spectroscopic study of reactions within rust layers. Corros. Sci. 29, 1329-1352.

Stroes-Gascoyne, S., C.J. Hamon, D.A. Dixon, C.L. Kohle, and P. Maak. 2007. The effects of dry density and porewater salinity on the physical and microbiological characteristics of compacted 100 % bentonite. In Scientific Basis for Nuclear Waste Management XXX, (D.S. Dunn, C. Poinssot, B. Begg, Editors), Mat. Res. Soc. Symp. Proc. 985, Materials Research Society, (Warrendale, PA), in press.

Tamaura, Y., K. Ito, and T. Katsura. 1983. Transformation of γ-FeO(OH) to Fe_3O_4 by adsorption of Iron(II) ion on γ-FeO(OH). Chemical Society Dalton Transformation, 189–194.

Taniguchi, N. 2003. Effect of magnetite as a corrosion product on the corrosion of carbon steel overpack. In Prediction of Long Term Corrosion Behaviour in Nuclear Waste Systems. European Federation of Corrosion Publication No. 36 (Institute of Materials, Minerals and Mining, London), p. 424–438.

Taniguchi, N., M. Kawasaki, S. Kawakami, and M. Kubota. 2004. Corrosion behaviour of carbon steel in contact with bentonite under anaerobic condition. In Prediction of Long Term Corrosion in Nuclear Waste Systems. Proc. 2nd Int. Workshop, Nice, September 2004 (European Federation of Corrosion and Andra), p. 24–34.

Tsuru, T., E.I. Fujii, and S. Haruyama. 1990. Passivation of iron and its cathodic reduction studied with a rotating ring-disk electrode. Corros. Sci. 31, 655-660.

Tsushima, T., N. Hara, and K. Sugimoto. 2003. Zairyo-to-Kankyo 51, 350.

Vela, M.E., J.R. Vilche, and A.J. Arvia. 1986. The dissolution and passivation of polycrystalline iron electrodes in boric acid-borate buffer solutions in the 7.5–9.2 pH range. J. Appl. Electrochem. 16, 490–504.

Wersin, P., L.H. Johnson, B. Schwyn, U. Berner, and E. Curti. 2003. Redox conditions in the near field of a repository for SF/HLW and ILW in Opalinus Clay. Nagra Technical Report, NTB 02-13.

Westerman, R.E., J.H. Haberman, S.G. Pitman, B.A. Pulsipher, and L.A. Sigalla. 1986. Corrosion and environmental-mechanical characterization of iron-base nuclear waste package structural barrier materials. Annual Report – FY 1984. Pacific Northwest Laboratory Report, PNL-5426.

Yoshikawa, H., E. Gunji, and M. Tokuda. 2008. Long stability of iron for 1500 years indicated by archaeological samples from the 6th Yamato ancient tomb. Extended abstract in Proc. 3rd Int. Workshop on Long-term Prediction of Corrosion Damage in Nuclear Waste Systems, Pennsylvania State University, State College, PA, May 14–18, 2007. To be submitted to J. Nucl. Mater.